EUROPEAN ORGANIZATION FOR NUCLEAR RESEARCH

CERN-EP/87-55
March 10th, 1987

CERN LIBRARIES, GENEVA

CM-P00062349

PERFORMANCE OF A URANIUM/TETRAMETHYLPENTANE ELECTROMAGNETIC CALORIMETER

M.Albrow[1], R.Apsimon[1], B.Aubert[2], C. Bacci[3], A. Bezaguet[4], R. Bonino[5], S.Centro[3], F.Ceradini[3], P. Cennini[4], C. Cochet[7], J.Colas[2], R. Conte[6], J.P. DeBrion[7], M. DeGiorgi[6], A. DiCiaccio[4], F. Diez-Hedo[8], J. Dowell[4,5], L. Dumps[4], Ph. Ghez[2], A.Givernaud[4], A. Gonidec[4], W. Kienzle[4], F. Lacava[3], A. Looten[4], T. Markiewicz[9], C. Markou[10], G. Maurin[4], A. Meneguzzo[6], Th. Müller[4], R. Munoz[4], L. Naumann[4], S. Ochsenbein*, E. Petrolo[4], C. Pigot[7], A. Placci[4], M. Pripstein[2], E. Radermacher[4], D. Robinson[10], C.Rubbia[4], J. Sass[4], D. Schinzel[4], W.F. Schmidt[4], C. Seez[10], W. Seidl[4], J. Streets[5], K. Sumorok[11], S. Veneziano[3], J. Virdee[10], E. Warmuth[12], L. Zanello[3]

ABSTRACT

A calorimeter, consisting of uranium plates and thin liquid ionization chambers filled with tetramethylpentane (TMP) at room temperature, has been tested using electrons between 10 GeV and 70 GeV. The essential characteristics of the liquid are discussed, including measurements of the free electron lifetime. Results on uniformity, linearity and energy resolution are described and some information on the response to hadrons has been obtained. A single TMP box containing four electrodes and a TMP position detector for electromagnetic showers have also been tested.

(Submitted to Nuclear Instruments and Methods in Physics Research)

1) Rutherford Appleton Laboratory, Didcot, UK
2) Annecy (LAPP), France
3) University of Roma "La Sapienza" and INFN, Italy
4) CERN, Switzerland
5) University of Birmingham, UK
6) University of Padova and INFN, Italy
7) Centre d'Etudes Nucléaires, Saclay, France
8) Junta de Energia Nuclear, Madrid, Spain
9) University of Wisconsin, USA
10) Imperial College, London, UK
11) University of Harvard, USA
11) Inst. für Hochemergiephysik der Österreich. Akad. Wissensch., Vienna, Austria.

* SIN, ETH Zurich, Switzerland

1. INTRODUCTION

A sampling calorimeter that uses, as active medium, a liquid ionization chamber has several advantages. The direct collection of the charge liberated by the passage of an ionizing particle is the most absolute and stable way of recording a signal, provided that the properties of the liquid remain constant. As thousands of ion pairs are typically created, their statistical fluctuations are negligible compared to sampling fluctuations. Futhermore, the calorimeter is spatially uniform, easy to segment in depth as well as surface, insensitive to magnetic fields and requires little space for readout cables. On the other hand, the signals are small and consequently accurately calibrated, low-noise amplifiers are needed.

Until now, liquid argon is the only liquid to have been used in a practical calorimeter. The use of a liquid that will operate at room temperature has the further advantage that cryogenic containers with their inherent dead spaces needed for insulation are avoided. A warm liquid calorimeter can therefore be more easily accommodated in a restricted or geometrically awkward space.

We describe here tests performed with two calorimeter modules consisting of uranium plates with Tetramethylpentane (TMP) as the active medium. The use of a hydrogenous liquid with uranium is expected, under certain conditions, to compensate for the difference in response between electrons and hadrons (e/π ratio) because recoil protons from the collisions of fission and spallation neutrons increase the hadron response[1]. The measurements were carried out as part of the improvement programme of the UA1 experiment at the CERN Proton-Antiproton collider in which the present lead-scintillator electromagnetic calorimeters are to be replaced by uranium and TMP[2]. This will give about 2.6 hadronic interaction lengths instead of the present one interaction length so that the calorimeters will be partly hadronic, for example absorbing on average about 90% of the energy of a 10 GeV hadron. Although the calorimeters described here were built primarily to detect electrons, as a test of the basic feasibility of the technique, some results pertaining to the hadron response have also been obtained.

The essential characteristics of any ionization chamber liquid are that it should have high enough yield, mobility and lifetime of free electrons to give satisfactory signal/noise, response time and reliability. Factors affecting the choice of the liquid are discussed in section 2. The technical details of the calorimeters, cleaning and filling procedures are described in section 3. Sections 4 and 5 give details of the experimental layout and the electronics. The performance of the calorimeters is discussed in section 6 and tests of a prototype TMP position detector are presented in section 7.

2. WARM LIQUIDS AND THE CHOICE OF TMP

The liquids that have been investigated so far and found to have suitable electronic properties are Tetramethylsilane (TMS, $(CH_3)_4Si$) [3], 2, 2, 4, 4 Tetramethylpentane (TMP C_9H_{20}) [4,5] and Hexamethylethylenedisilane (HEDS) [6], familiarly called Double TMS (Table 1). These liquids have a non-polar molecular structure, an absence of reactive groups (Cl, O, OH, etc.), and support the existence of free electrons at room temperature. In addition, electrons produced through ionization can easily be drifted in them by applying an external electric field. Owing to the high flammability of TMS (boiling point = 26.5^0C, flash point = -18^0C) preference is given to liquids with higher boiling and flash points. TMP and HEDS are therefore better candidates. We have chosen TMP because of the lower electron yield of HEDS (Table 2).

Table 1 -STRUCTURE FORMULAE

a) TMS

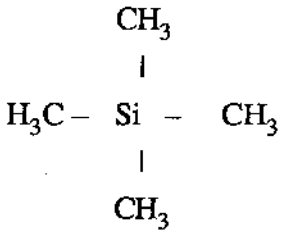

b) TMP

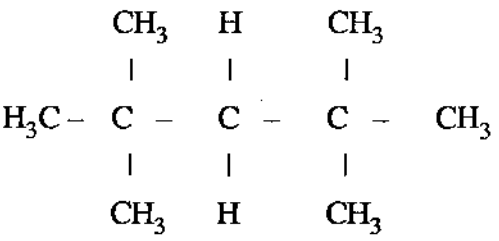

c) HEDS

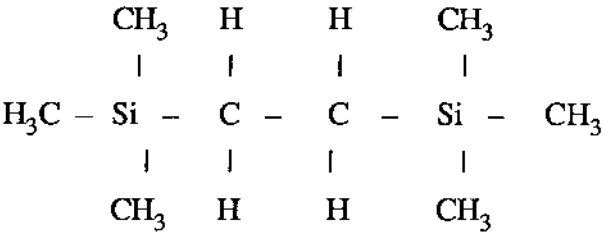

The properties of a liquid that are relevant for calorimetry are the yield of free ion pairs per unit energy deposition, $G_{fi}(E)$, the electron mobility, μ, and the electron lifetime, τ. The factors that affect these quantities are discussed in more detail in reference 7.

$G_{fi}(E)$ is determined by recombination phenomena and increases with increasing electric field, E. The problem has been treated theoretically by Onsager[8]. To first order in E, $G_{fi}(E)$ is given by

$$G_{fi}(E) = G_o\,(1 + e_o^3\,E/8\,\pi\epsilon_o\,\epsilon\,k^2T^2)$$

where G_o is the yield of ion pairs at zero field, e_o is the electronic charge, and the other symbols have their usual meanings. Fig. 1 shows the product of $G_{fi}(E)$ and specific energy loss (dE/dx) for a minimum ionizing particle in TMP compared to liquid argon, including higher powers of E.

The electron mobility, μ, determines the drift or transit time, t_d, across the liquid gap, d;

$$t_d = d/\mu E \qquad (2.1)$$

Fig. 2 shows the dependence of t_d on the electric field for a gap of 1.25 mm in TMP. At low fields (<100 V/cm) the mobility of electrons in liquid argon (~500 cm^2/Vs) is much larger than in TMP (~30 cm^2/Vs). However, because of saturation effects in liquid argon [9], the drift velocity of electrons is the same (~3 mm/μs) in both liquids at 10 kV/cm. The mobility of the positive ions is several orders of magnitude lower and their contribution to the detected pulse can be neglected.

The finite electron lifetime, τ, is caused by the presence of electron capturing impurities or scavengers. For low free electron yields compared to the density of scavenger molecules, the number of electrons decreases exponentially as a function of time

$$n = n_o\, e^{-t/\tau}$$

Fig. 3 shows electron lifetimes in TMS for several scavengers of interest. No measurements have been performed up to now on TMP, but as the capture rates scale with mobility it is expected to be roughly three times less sensitive to impurities.

The foremost problem in producing a suitable liquid is the exclusion or removal of electron attaching impurities during production. Experience has shown that careful attention must be paid to the choice of the raw materials used. TMS and TMP produced commercially under the above conditions have achieved the necessary purity. All three liquids in Table 2 have shown electron lifetimes exceeding 20 μs, after a final cleaning using activated silica-gel and molecular sieves[7].

Table 2 : Properties of Room Temperature Calorimeter Liquids

	TMS	TMP	HEDS
Density (g/cm^3)	0.645	0.72	~0.75
dE/dx (MeV/cm)	1.36	1.58	~1.60
G_{fi} (ion pairs per 100 eV) at 15 kV/cm	1.42	1.37	0.76
Mobility (cm^2/Vs)	100.	30.	45
Vapour Pressure (torr at 20°C)	650.	15.	<10.
Flashpoint (°C)	-18	+7	~10
Boiling point (°C)	26.5	122.	150.
Dielectric Constant	1.84	1.98	--

3. THE TEST CALORIMETERS

3.1 Technical details

Two calorimeters have been constructed, one with 4 mm thick uranium plates and one with 2 mm plates. Each consists of a stack of 20 flat, square boxes filled with TMP with alternate uranium plates. As shown in Fig. 4 the stack is held together between two thick frames by aluminium bars leaving a window with an opening of 11 cm x 11 cm which covers the size of the sensitive volume inside the boxes.

Each box (Fig. 5) measures 11.5 cm x 11.5 cm with a total thickness of 3.3 mm, and is made of stainless steel frame, 3 mm thick, on which two 150 μm stainless steel foils have been laser welded. Inside the box a 500 μm thick central electrode is held by five ceramic spacers. The feed-through for high voltage (which connects to the electrode) and two 2 mm pipes for filling are welded into the frame. The nominal liquid gap is 1.25 mm with an uncertainty of 0.1 mm due to the deformation of the foils under the pressure of the liquid and the flatness of the uranium plates.

The inlet and outlet pipes of all 20 boxes, arranged on the top in the experimental set up, are connected together via two manifolds which are closed with two valves after filling.

The signal outputs of 5 consecutive boxes are connected to one channel in the readout system giving four channels for each calorimeter. Because of damaged insulation inside the HV feedthroughs, a few of the boxes were not connected. The uranium plates in front of them were replaced by aluminium plates.

A summary of technical data of the calorimeters is given in Table 3.

TABLE 3

Absorber :		
Square plates of depleted uranium, 4 mm or 2 mm thick :	1.25 or 0.63	Xo
Material of the boxes : 0.8 mm steel, 2.5 mm TMP :	0.045	Xo
Total (allowing for missing uranium plates) :	22.3 or 12.9	Xo
Detector :		
Ionization box :	115 mm x 115 mm x 3.3 mm stainless steel	
Electrode :	103 mm x 103 mm x 0.5 mm " "	
Feedthrough :	Friedrischsfeld 3.9 mm diameter, with adapter	
Liquid :	Tetramethylpentane 2 x 1.25 mm	
Operating parameters :		
Nominal operating voltage during tests :	1250 V = 10 kV/cm	
Transit time at 10 kV/cm :	416 ns	
Capacitance per box :	360 pF	

3.2 Cleaning procedure

Before welding, all stainless steel surfaces were cleaned by the following procedure :

- degreasing in perchlor-ethylene vapour (~10 min)
- ultrasound bath in water with a few % almeco (detergent) (~15 min)
- rinsing in demineralized water (few min)
- vacuum baking at 950^0C (few hours).

Initial tests with the 4-mm plate calorimeter gave an unacceptably short electron lifetime which was measured by the methods described in section 6.1. After eliminating the possibility that the TMP had become contaminated with oxygen during filling (section 3.3) samples of the metal surfaces of the boxes were subjected to an Auger electron analysis [10] which measures the atomic fractions of the first few atomic layers (Fig. 6). The oxygen is assumed to be in the form of iron-oxide. However, traces of sulphur and chlorine were found at the few % level (Fig. 6a) that would be sufficient to account for the decrease of the lifetime if dissolved in the TMP. An additional cleaning was therefore performed inside the assembled boxes :

- flushing the boxes with 60^0C acetone (3 hours)
- flushing with 60^0C ethylalcohol (3 hours)
- flushing with ultra-pure 80^0C water (36 hours)
- ultrasound during the whole operation
- drying with hot helium (3 days).

Ultra-pure water (impurities of few ppb) has been used at CERN for cleaning the surfaces of super-conducting RF cavities developed for LEP. The resistivity of the water used here was 18 MΩcm. Its high dielectric constant (~80) makes it very effective for removing polar molecules.

As a result the amount of surface pollution was reduced by a factor of about 5 (see Fig. 6b) and there was no measurable reduction in the electron lifetime after filling (see also section 6.1). A more complete description of the surface treatment can be found in reference 10.

3.3 Filling procedure

The principles of the filling method are shown in Fig. 7. The calorimeter was placed in a large vacuum vessel. For safety reasons aluminium plates were placed between the boxes during filling. The calorimeter and the vessel were evacuated to avoid a pressure differential and consequent collapse of the boxes. The calorimeter was then heated to 300^0C and pumped until the residual pressure, measured at the entrance of the pump, reached 10^{-7} torr. Note that because of the long thin filling pipes (1 mm internal diameter) the pressure in the boxes was considerably higher than the measured value. After cooling, the calorimeter was filled by opening the valves to the TMP container. The valves were then closed and the capacitances of the boxes measured to verify that they were full. Finally the aluminium plates were replaced by uranium and the calorimeter placed in an electrically and acoustically well shielded box (Faraday cage).

4. TEST BEAM AND EXPERIMENTAL LAYOUT

Tests were carried out at the CERN SPS using a tertiary beam with a maximum momentum of 80 GeV/c and $\Delta p/p$ of 0.3% after measurement with a beam spectrometer. A rather clean and narrow ($\pm$ 2 mm) electron beam in the 10-70 GeV range was obtained using a thin (4 mm) lead target, the electrons originating from the bremsstrahlung loss of 80 GeV electrons in the parent beam. Fig. 8 shows the experimental layout.

Delay-line wire chambers were used to define the incident particle position and direction to better than 1 mm and 0.1 mrad respectively. The test calorimeters were followed by an Iron/Scintillator calorimeter, a prototype of the present UA1 hadron calorimeter C-modules [11], and 160 cm of Iron. Data were taken with electrons, hadrons and muons between 10 and 70 GeV. For electron runs, 10 cm of lead were placed in front of the scintillation counter M1 which was used in anti-coincidence with $S_2S_3\ \overline{V}$ to remove pions and muons. The absence of a signal in the hadron calorimeter was also required off-line. For muons, M_1M_2 were used in coincidence and the beam defocussed to cover the area of the test calorimeters.

In addition to the two calorimeters, a single 4-electrode box[12] and a position detector[13], both using TMP, were also tested. Details of these items are given later.

5. ELECTRONICS AND NOISE LEVEL

As shown in Fig. 1, the primary electron yield for TMP is only about 30% of that for liquid argon at 20 kV/cm. Consequently the amplifier noise is even more critical in our case. A full discussion of the considerations that led to the adoption of the scheme used here is given elsewhere[14]. The r.m.s. noise is dominated by the capacitance of the detector (serial noise) which is about 2 nF for a set of 5 boxes. Rather than try to match the capacitance of the detector to that of the amplifier using a transformer[15], the approach has been to use four low noise jFETs with high transconductance, g_m, in parallel[14]. The signal/noise ratio (S/N) for a minimum ionizing particle is determined by :

$$S/N \sim q_{mip}(ng_m)^{1/2} / (nC_{amp} + C_D)$$

where n is the number of jFETs, q_{mip} is the charge resulting from the passage of a minimum ionizing particle, C_{amp} is the amplifier input capacitance (75 pF per jFET) and C_D the detector capacitance. Fig. 9 shows the measured noise as a function of C_D for 1, 2 and 4 jFETs in parallel.

A hybrid pre-amplifier with four jFETs has been constructed[14]. In the tests the amplifiers were placed close to the detectors (Fig. 10), and connected by 10 m long shielded coaxial cables to shaping amplifiers with a shaping time of 2 μs[14]. Lecroy 2282 ADCs were used to digitize the pulses and calibration was performed using test pulses of accurately known charge. Fig. 11 shows the noise characteristics for a typical hybrid. About 3000 electrons noise are expected for a 5-box unit. At 10 kV/cm the S/N expected is 3:1 for a minimum ionizing particle.

However, with uranium plates between the boxes, the r.m.s. noise is increased further by uranium radioactivity which, because of its random timing and the AC coupling, does not produce a net signal. Fig. 12 shows the measured noise as a function of the applied electric field for two 5-box channels. At 10 kV/cm the noise is increased by about 40% showing that the uranium contributes approximately equally. Fig. 13 shows typical pulse height spectra for muons and pedestal. The S/N ratio is about 2:1.

6. PERFORMANCE OF THE CALORIMETER

6.1 Measurement of the lifetime of electrons in the liquid

The lifetime of electrons in the TMP and its stability as a function of time are both critical parameters in the performance of the calorimeters. The lifetime must be long enough to ensure that most of the electrons are collected and must remain constant to the extent that time-dependent corrections are unnecessary.

By operating at low fields, where the transit time of the electrons (equation 2.1), is long compared to their lifetime, more electrons are captured before they reach the anode. This alters the shape of the charge pulse compared to that from an ideal ionization chamber and results in a lower total collected charge. Both effects have been used to estimate the lifetime. The collected charge as a function of time (pulse shape) is given by [5].

$$Q(t) = Q\ \tau/t_d\ [(1-\ \tau/t_d)\ (1-e^{-t/\tau}) + t/t_d\ e^{-t/\tau}]\quad \text{for } t<t_d \qquad (6.1)$$

and the full collected charge :

$$Q(\ t_d\ ) = Q\ \tau/t_d\ [\tau/t_d\ \ (e^{-t_d/\tau}-1) +1]\quad \text{for } t=t_d \qquad (6.2)$$

where Q is the initial charge carried by ionization electrons.

Method 1 (Total charge)

The effect of the finite lifetime on the total collected charge $Q(t_d)$ is determined by the factor

$$\tau/t_d\ [\tau/t_d(e^{-t_d/\tau}-1) + 1] \qquad (6.3)$$

in equation 6.2 and tends to 1/2 for lifetimes long compared to t_d which is a function of the electric field. However, as discussed in section 2, because of electron-ion recombination the total ionization yield Q also depends on the electric field and in a linear approximation is given by[8)]

$$Q = Q_o(1+\alpha E) \qquad (6.4)$$

where for the present case $\alpha = 0.057$ cm/kV and $Q_o = 2900$ electrons for a minimum ionizing particle passing through one box. Thus, the determination of τ by this method is sensitive to the correctness of the assumed dependence of Q on the electric field (Onsager theory[8)]).

The calculated form of $Q(t_d)$ versus **E** is shown in Fig. 14 for various lifetimes from which it is clear how the shape of the curve can be used to measured the lifetime. A two-parameter fit gives Q_o(normalization) and τ, after corrections are applied for the amplifier response[5)]. In practice, a somewhat better χ^2 results from including a quadratic term in **E** in equation 6.4 and such fits were made to obtain the lifetimes quoted below using 70 GeV electrons. Because of the sensitivity to the details of the Onsager theory, lifetimes determined by this method are considered less reliable than those obtained using the pulse shape method discussed below. This is particularly true for long lifetimes (>10μs). However, short lifetimes (≤ 1 μsec) are easily recognized as they produce marked departures from the Onsager shape (Fig. 14). A typical fit for the 4-mm calorimeter is shown in Fig. 15a, yielding a lifetime of 5±1 μs. The purity of the liquid used to fill the 2-mm calorimeter was higher and Fig. 15b shows a typical fit for this case giving $\tau = 27\pm4$ μs. Because of the longer lifetime this measurement was performed using the preamplifier output (Fig. 10) to minimize the amplifier response correction whereas the 4-mm calorimeter measurement used the output of the shaper. The errors given on the lifetimes are statistical.

Method 2 (Pulse shape)

When the transit time is much larger than the lifetime, the time evolution of the pulse is especially sensitive to the lifetime. The collection of charge ends when all electrons have been absorbed by impurities before they reach the anode.

The lifetime is determined by fitting the observed pulse shape after the preamplifier with equation 6.1 convoluted with the amplifier response function [5)]. The first measurements were made with 60 V applied voltage (0.5 kV/cm) which gives a transit time of 8.7 μs. A typical pulse shape and superimposed fit for a 70 GeV electron are shown in Fig. 16a for the 4-mm plate calorimeter, yielding a lifetime of 2.9±0.5 μs. The improved purity of the liquid used in the 2-mm plate calorimeter necessitated even lower fields and the result (14±3 μs) shown in Fig. 16b was obtained with 17 V. Repeated measurements gave lifetimes of a few μs for all cells in the 4-mm plate calorimeter and in excess of 10 μs for the 2-mm plate calorimeter, broadly consistent with those found using Method 1.The errors given are statistical.

6.2 Stability of the calorimeter response

In order to be useful for practical calorimetry the purity of the liquid and hence the reponse of the calorimeter should be stable over a period of years. Recirculation of the liquid is not planned. Quantitatively, any time dependent corrections should be kept less than 1% for the performance to be considered satisfactory. With an electric field of 10 kV/cm (t_d = 416 ns) and a lifetime of 3 μs the fraction of charge collected, given approximately by (1 - 1/3 t_d/τ), is about 95%. With a 30 μs lifetime it is 99.5%. Meaningful stability checks have been possible only with the 4-mm plate calorimeter because the 2-mm plate version was available only for a short time. In fact no measureable degradation of either the lifetime or the pulse height (at the percent level) have been observed over a three-month period suggesting that both the cleaning procedures and the sealing of the boxes are adequate.

6.3 Spatial uniformity

Measurements of the average pulse height distribution across a single box (Fig. 17) and the average response of each of the 17 connected boxes (Fig. 18) in the 4-mm plate calorimeter were made using 70 GeV muons. In both cases the root mean square deviation is about 5%. Fig. 20 shows the spatial variation of the pulse height across the four-electrode single box [12] (Fig. 19) for a 70 GeV electron shower generated with 1 cm of lead. The summed pulse height across the inter-electrode gap is uniform and the cross talk, when the beam is centred on one of the electrodes, is less than 1%.

6.4 Linearity and energy resolution for electrons

In order to obtain a clean electron signal, events were accepted and analysed only if they satisfied the following conditions :

1 - Cuts on beam momentum spread

2 - Size of the beam spot limited to 2 cm in the horizontal direction and 5 cm in the vertical direction.

3 - No response from the veto counter V (at least part of events with accompanying halo are suppressed)

4- No response from the two muon counters M1 and M2 or from the hadronic calorimeter. M1 was preceded by 10 cm of lead.

These cuts removed about 30% of all recorded events.

As the 2-mm plate calorimeter has only 12.9 radiation lengths of material it does not fully contain electromagnetic showers and account must be taken of the thicker plates in the following 4-mm plate calorimeter in order to estimate the energy resolution that would be obtained with an electromagnetic calorimeter made only of 2-mm plates.

Measurements were made with electrons between 10 and 70 GeV. The recorded charge for each of the electronic channels was weighted with an individual energy-independent calibration constant obtained by minimizing the resolution, using the beam spectrometer to measure the electron momenta, and then summed over the two calorimeters. The weighting factors are given in Table 4. Pulse height spectra at three energies are shown in Fig. 21, and the average pulse height as a function of depth in Fig. 22. The pulse heights in the 4-mm section have been doubled to allow for the different sampling frequency. Fig. 23 shows the average total pulse height as a function of electron energy. The deviations from the fitted straight line are less than 0.2%. The measured resolution as a function of electron energy is given in Fig. 24. The solid lines are for $\Delta E/E = 0.12/\sqrt{E}$ and $0.14/\sqrt{E}$. The slight worsening of the resolution with increasing energy is due to the increasing fraction of the showers occuring in the rear 4-mm section (see Fig. 22).The dashed curve is an estimate of the resolution that would be expected for the combined 2-mm and 4-mm calorimeters if the intrinsic resolution of a 2-mm calorimeter were $0.12/\sqrt{E}$. The results are consistent with a resolution close to $0.12/\sqrt{E}$ if allowance is also made for the beam momentum resolution of $\pm$ 0.3%. This result is in good agreement with a Monte Carlo prediction ($0.118/\sqrt{E}$) using the GEANT simulation [16].

Table 4

Weighting factors for each calorimeter cell used to minimize the resolution

2-mm cal. cell	1	1.000*
	2	0.980
	3	0.912
	4	1.122
4-mm cal. cell	1	1.966
	2	1.993
	3	1.939
	4	2.034

* The weights are normalized to that of the first cell.

6.5 Response to hadrons

As already mentioned, the use of uranium with TMP is expected to increase the hadron response relative to that for electrons because fission and spallation neutrons produce recoil protons in the TMP[1].

The calorimeters described here were not designed to contain hadronic showers, neither laterally nor in depth. The lateral energy leakage is expected to be about 25%. Nevertheless, an idea of the response to hadrons and consequently of the e/π response ratio has been obtained by comparing the observed pulse height distribution for incident hadrons with that predicted by the GEANT Monte Carlo program using the GHEISHA code [16] assuming a Birk's constant K_B of 0.014 cm/MeV[17], close to that for PMMA scintillator[1]. This constant parametrizes the saturation of the ionization for highly ionizing particles by the expression

$$(dE/dx)_{eff} = dE/dx / (1 + K_B\, dE/dx)$$

The energy calibration is taken from the electron data. Figs. 25 and 26 show the results for 50 GeV and 70 GeV pions respectively. The solid curves are the predictions and agree rather well with the data. The same Monte Carlo program, applied to the planned UA1 upgraded calorimeter, predicts an e/π ratio very close to unity. A Birks' constant of 0.020 cm/MeV is clearly in much worse agreement with the data (Fig. 25). As a check that recoil protons are really playing a significant part, the dashed curve in Fig. 25 shows the effect of removing the fission process in the Monte Carlo.

These results give us confidence that the upgraded UA1 calorimeter will have good hadronic energy resolution which is predicted by the Monte Carlo program to be $0.46/\sqrt{E} + 0.04$.

7. A POSITION DETECTOR USING TMP

The possibility of using a TMP cell with smaller electrodes as a position detector for electromagnetic showers has been tested[13]. A 10 x 10 cm^2 box, similar to those used in the calorimeters, was equipped with eight 10 mm wide electrodes having a pitch of 13 mm (Fig. 27). The positions of the incident electrons were measured to $\pm$ 0.5 mm with a wire chamber and showers were generated with various thicknesses of lead. Typical distributions of the average pulse height in each electrode of the position detector are shown in Fig. 28. In Fig. 28b the beam position has been moved by 1 cm. The shower position is calculated as the centroid of the pulse height distribution for a single event. Fig. 29a shows the correlation between the position measured by the wire chamber and that measured by the position detector. The difference between the two measurements (residual) is plotted in Fig. 29b from which the position resolution can be deduced. The resolution has been studied as a function of the lead thickness and the electron energy (Fig. 30). Best results are obtained for lead thicknesses greater than about 4 radiation lengths giving a r.m.s. resolution of better than 2 mm for energies greater than 40 GeV.

8. CONCLUSIONS

We have described measurements made with two electromagnetic calorimeters consisting respectively of 2-mm and 4-mm uranium plates interleaved with 10x10 cm^2 boxes containing 2.5 mm of Tetramethylpentane (TMP).

The following results have been obtained :

Lifetimes of electrons in TMP have been observed that are adequate for calorimetry, i.e. greater than ten microseconds to be compared to an electron transit time across the liquid gap of a few hundred nanoseconds, which means that more than 99% of the charge produced by the passage of an ionizing particle is collected. Furthermore, no deterioration has been found over a period of more than three months. These results show that adequate cleaning procedures have been achieved that are able to reduce the level of electronegative impurities in the TMP to an acceptable level with no measurable long term release of such impurities. Equally, the use of sealed boxes to contain the TMP seems to be viable.

Amplifiers with sufficiently low noise level (~3000 electrons) have been constructed giving a signal/noise ratio of 3:1 for a minimum ionizing particle passing through 5 TMP boxes which becomes 2:1 in the presence of uranium radioactivity.

Variations of the pulse height across a single TMP box and from box to box are both at the 5% level which is sufficient for high quality calorimetry.

The response of the combined calorimeters to electrons is linear to within 0.2% while the energy resolution varies from $0.12/\sqrt{E}$ at 10 GeV to $0.14/\sqrt{E}$ at 70 GeV. These results are consistent with a resolution of $0.12/\sqrt{E}$ for a calorimeter composed entirely of 2 mm thick uranium plates and are in agreement with Monte Carlo predictions.

Measurements with incident hadrons, whose energy is not fully contained, are also in agreement with Monte Carlo predictions and suggest that fission and spallation neutrons producing recoil protons in the TMP play an important role. They imply that the calorimeter planned for the upgraded UA1 detector should have an e/π response ratio close to unity and hence a rather good hadronic energy resolution.

A single TMP box containing four electrodes shows uniformity of the total pulse height when an electron shower is scanned across an inter-electrode gap and less than 1% cross talk between electrodes when the beam is centred on one electrode.

A TMP position detector containing 1 cm wide electrodes is able to measure the position of high energy electron showers to a precision of 2 mm.

ACKNOWLEDGEMENTS

We wish to acknowledge the support of the many individuals who have helped with this project, both inside and outside the UA1 Collaboration. In particular we mention the contribution of the electronic workshop of INFN-Sezione di Roma. In addition to CERN the following funding agencies have contributed to this programme :

Fonds zur Förderung der Wissenschaftlichen Forschung, Austria.

Institut National de Physique Nucléaire et de Physique des Particules and Institut de Recherche Fondamentale (CEA) France.

Istituto Nazionale di Fisica Nucleare, Italy

Junta de Energia Nuclear, Madrid, Spain.

Science and Engineering Research Council, United Kingdom.

Department of Energy, USA.

REFERENCES

1) R. Wigmans, CERN/EF 86-18, submitted to Nucl. Inst. and Methods.

2) J.D. Dowell, CERN-EP/86-193, to be published in proceedings of the 6th Topical Workshop on Proton-Antiproton Collider Physics, Aachen, 1986.

3) W.F.Schmidt and A.O.Allen, J.Chem.Phys.**52**(1970)4788

4) T.G.Ryan and G.R.Freeman, J.Chem.Phys.**58**(1978)5144.

5) C.Bacci et al., UA1 Technical Note TN 86-85 (1986) (unpublished).

6) A.Gonidec et al., UA1 internal memorandum (unpublished)

7) A. Gonidec et al., to be published.

8) L.Onsager, Phys.Rev.**54**(1938)554.

9) R.A. Holroyd and D.F. Anderson, Nucl. Inst. and Meth. **A236** (1985) 294-299.

10) Th. Muller et al., UA1 Technical Note, TN 86-92 (1986) (unpublished).

11) M.J. Corden et al., Nucl. Inst. and Meth. **A238** (1985) 273-287.

12) B.Aubert et al., UA1 Technical Note, TN 86-90 (1986) (unpublished).

13) M. Albrow et al., UA1 Technical note, TN 87-14 (1987) (unpublished).

14) C.Bacci et al., UA1 Technical Note, TN 86-112 (1986) (unpublished).

15) W. J. Willis and V. Radeka, Nucl. Inst. and Meth. **120** (1974) 221.
E. Gatti et al., Nucl. Inst. and Meth. **193** (1982) 539.

16) A.Givernaud, UA1 Technical Note, TN 86-109 (1986) (unpublished).

17) J.B.Birks, The theory and practice of scintillation counting (Macmillan, New York, 1964).

Figure Captions

Figure 1 : The free electron yield produced by a minimum ionizing particle in liquid argon and TMP as a function of the applied electric field (Onsager curves).

Figure 2 : The time taken for an electron to cross a 1.25 mm gap in TMP (transit time or drift time) as a function of the applied electric field.

Figure 3 : Electron lifetimes in TMS as a function of impurity concentration for various impurities.

Figure 4 : Constructional details of the U/TMP electromagnetic calorimeters.

Figure 5 : Details of a single TMP box.

Figure 6 : Auger electron spectrum of stainless steel boxes :
a) after standard cleaning procedures.
b) after additional cleaning including ultra-pure H_2O.

Figure 7 : The system used for filling the calorimeters with TMP.

Figure 8 : The experimental layout in the test beam.

Figure 9 : Equivalent noise charge of preamplifiers, equipped with 1, 2 and 4 jFETs in parallel, as a function of detector capacitance.The noise is measured after the shaping amplifier (Fig. 10).

Figure 10 : Schematic layout of the electronics used in the beam tests.

Figure 11 : Equivalent noise charge of a typical hybrid amplifier as a function of detector capacitance.The noise is measured after the shaping amplifier (Fig. 10).

Figure 12 : Noise of a hybrid preamplifier connected to 5 TMP boxes with uranium plates as a function of electric field.The noise is measured after the shaping amplifier (Fig. 10)

Figure 13 : Typical muon and pedestal pulse height spectra for a set of 5 boxes with uranium plates. The signal is 2.1 times the r.m.s. noise.

Figure 14 : Expected collected charge (electrons) for a minimum ionizing particle passing through a single TMP box as a function of applied electric field for various electron lifetimes (Onsager curves).

Figure 15 : Fit to the total collected charge versus electric field for a set of 5 boxes exposed to 70 GeV electron showers. The normalization and electron lifetime (τ) are free parameters. a) 4-mm plate calorimeter, b) 2-mm plate calorimeter.

Figure 16 : Fit to the collected charge as a function of time (pulse shape). The normalization and electron liftime (τ) are free parameters. a) 4-mm plate calorimeter, b) 2-mm plate calorimeter.

Figure 17 : The average muon pulse height distribution across a single box.

Figure 18 : The average response to muons of each of the (17) connected boxes in the 4-mm plate calorimeter.

Figure 19 : Schematic view of the 4-electrode box.

Figure 20 : Scan of an electron shower across the 4-electrode box shown in Fig. 19. The curves show the pulse height distribution for each of the two electrodes scanned. The point

at the centre is the summed pulse height.

Figure 21 : Pulse height spectra in the combined calorimeter for electrons at three energies.

Figure 22 : Depth profiles of the average energy deposition of electron showers in the combined calorimeter for various electron energies.

Figure 23 : The response of the combined calorimeters to electrons of various energies.

Figure 24 : The square of the measured energy resolution of the combined calorimeters as a function of electron energy. The solid and dot-dashed lines are for $\Delta E/E = 0.12/\sqrt{E}$ and $0.14/\sqrt{E}$ respectively where E is in GeV. The dashed line is the expected result if the resolution of a calorimeter made entirely of 2 mm plates were $0.12/\sqrt{E}$.

Figure 25 : Average pulse height spectrum for a 50 GeV π^+ incident on the combined calorimeter. The energy calibration is taken from the electron data. The solid (dot-dashed) curve is a Monte Carlo prediction for a Birk's constant of 0.014 (0.020) cm/MeV. The dashed curve shows the effect of removing the fission process in the Monte Carlo prediction.

Figure 26 : The same as Figure 25, but for 70 GeV π^+.

Figure 27 : Schematic design of the TMP position detector.

Figure 28 : a) The average pulse height per electrode of the position detector for electron showers of 70 GeV (beam width ± 2 mm).
b) The same, but with the beam displaced by 1 cm.

Figure 29 : a) The centroid of the position detector pulse height distribution plotted against the measured beam particle position for each event.
b) The difference between the two measurements of Figure 29a.

Figure 30 : a) The position detector resolution for showers generated with 2.5 cm of lead as a function of electron energy.
b) The position detector resolution for 30 GeV showers as a function of the thickness of lead used to generate them.

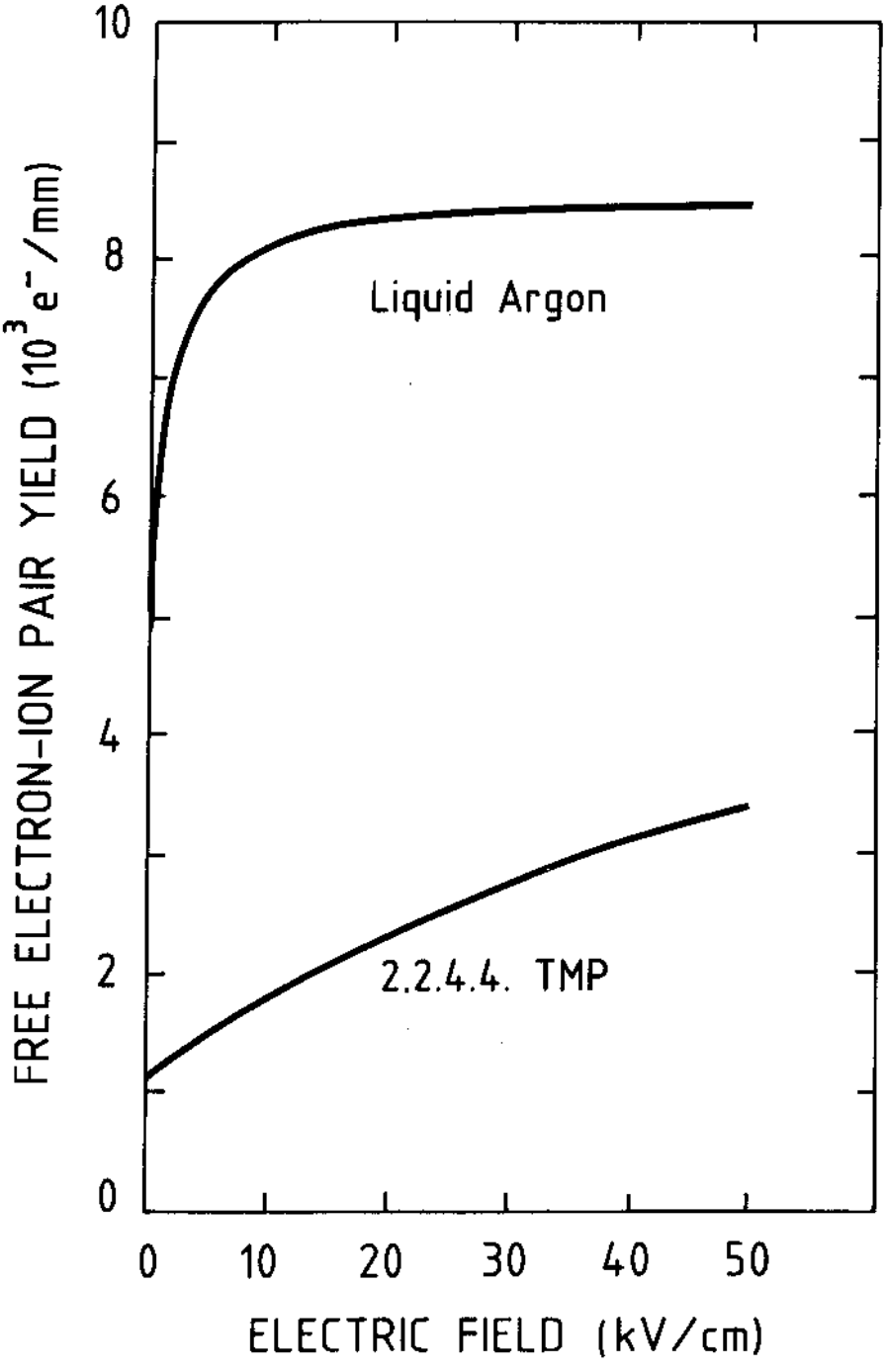
FREE ELECTRON-ION PAIR YIELD ($10^3 e^-$/mm)
10
8
6
4
2
0
Liquid Argon
2.2.4.4. TMP
0
10
20
30
40
50
ELECTRIC FIELD (kV/cm)

Figure 1

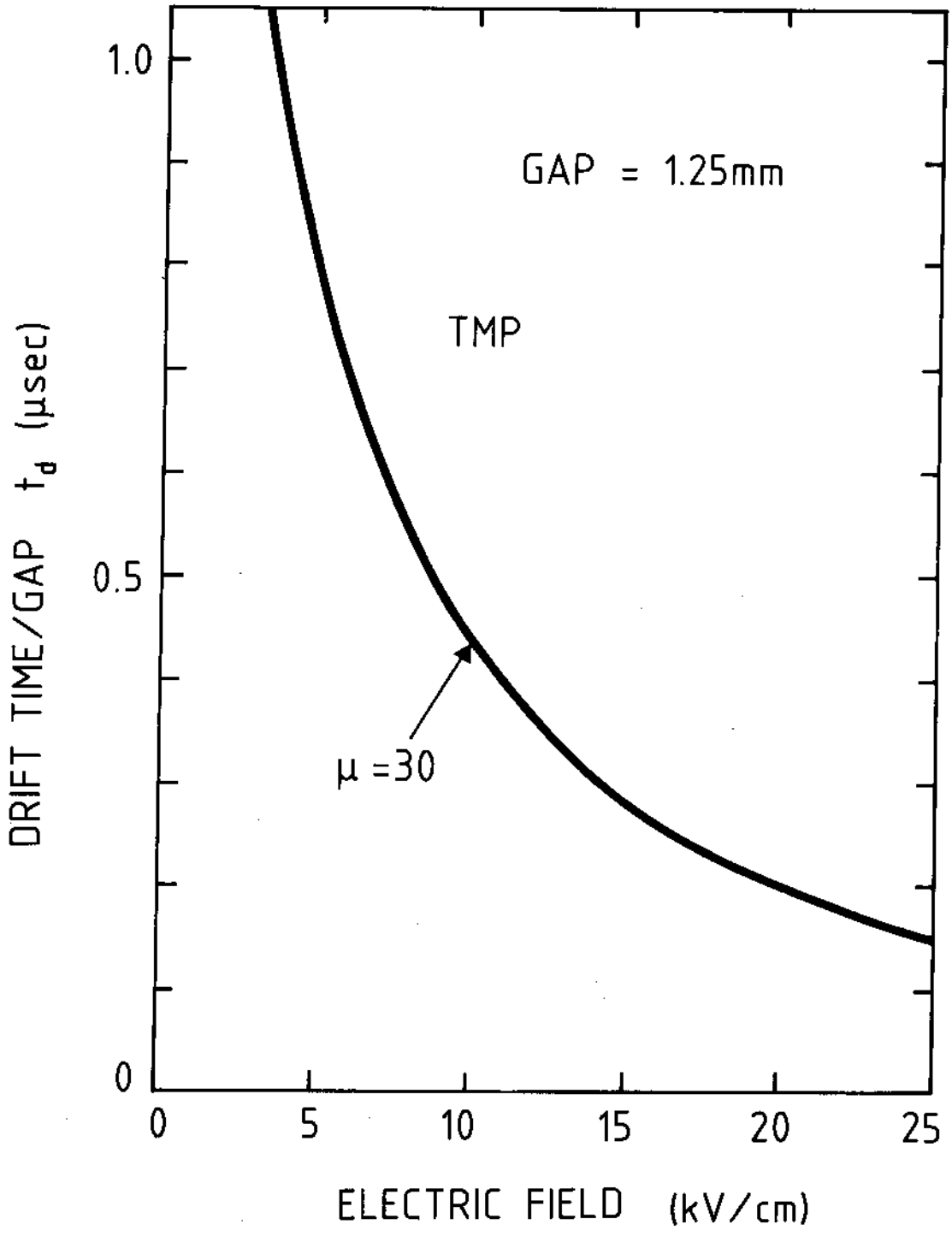
1.0
0.5
0
0
5
10
15
20
25
GAP = 1.25mm
TMP
μ =30
DRIFT TIME/GAP t_d (μsec)
ELECTRIC FIELD (kV/cm)

Figure 2

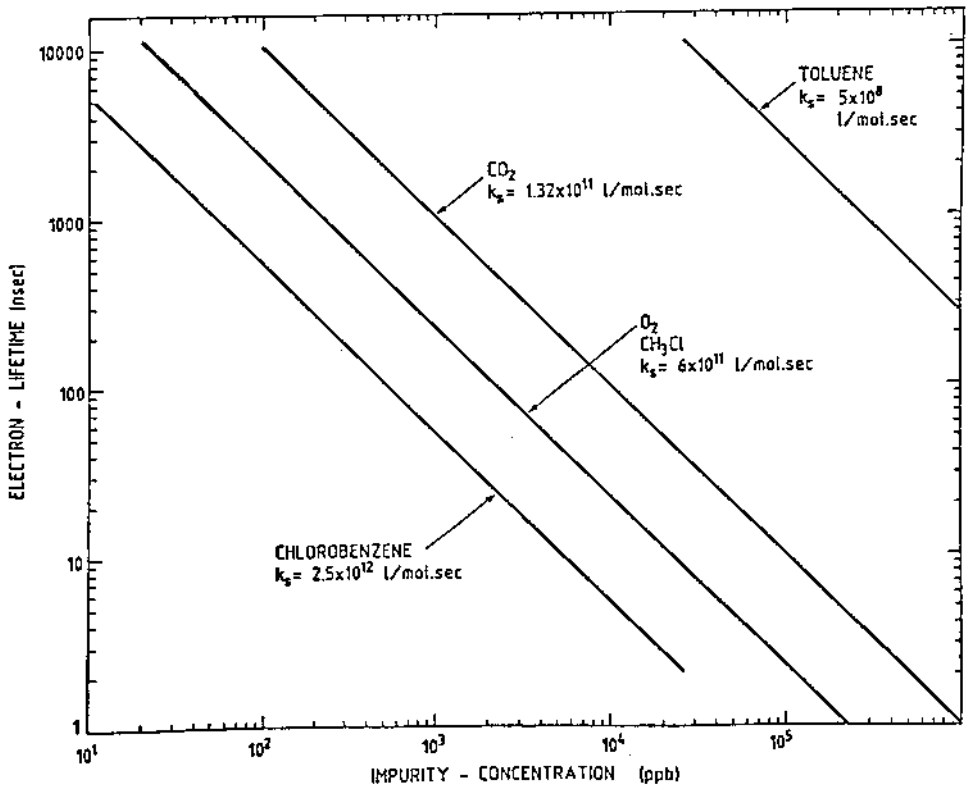
10000
1000
100
10
1
ELECTRON - LIFETIME (nsec)
10^1
10^2
10^3
10^4
10^5
IMPURITY - CONCENTRATION (ppb)
TOLUENE
k_e= 5x10^8
l/mol.sec
CO_2
k_e= 1.32x10^{11} l/mol.sec
O_2
CH_3Cl
k_e= 6x10^{11} l/mol.sec
CHLOROBENZENE
k_e= 2.5x10^{12} l/mol.sec

Figure 3

TEST CALORIMETER

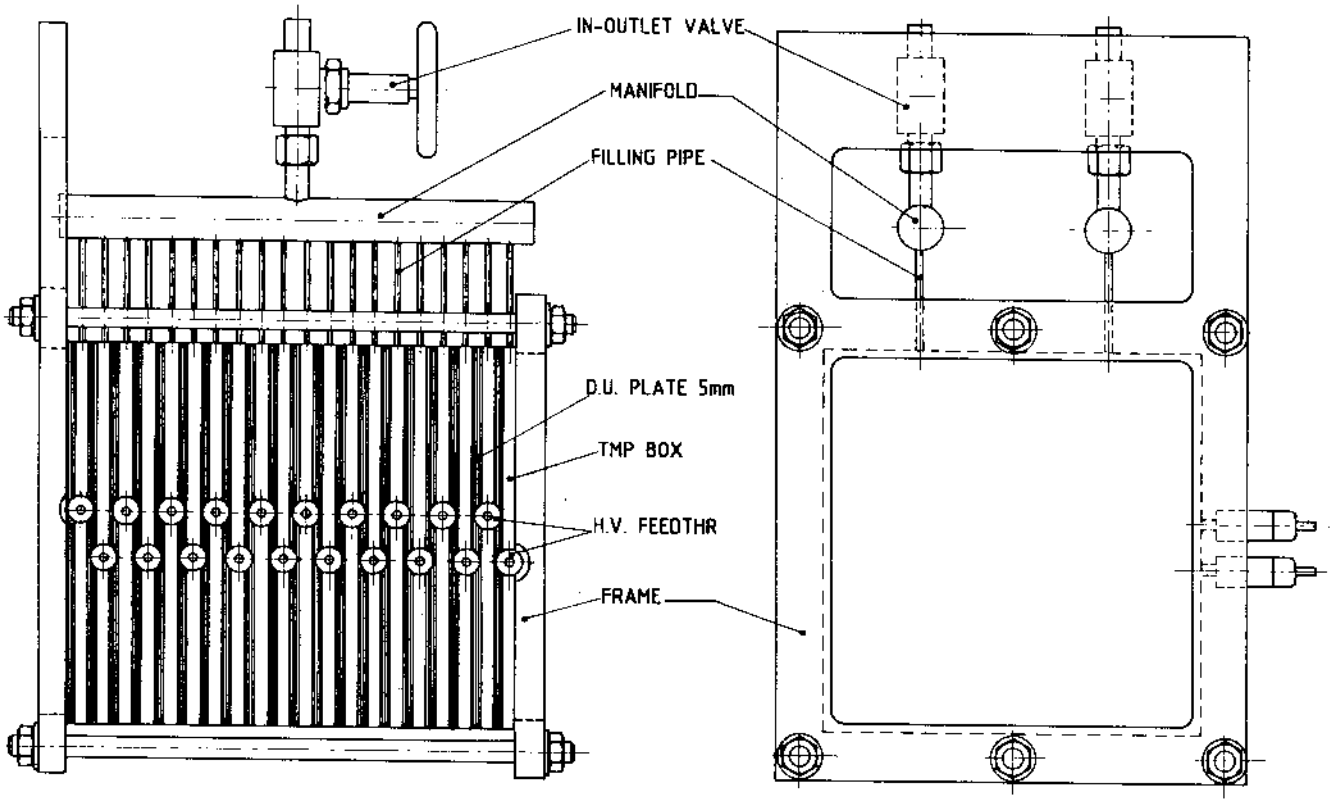

Figure 4

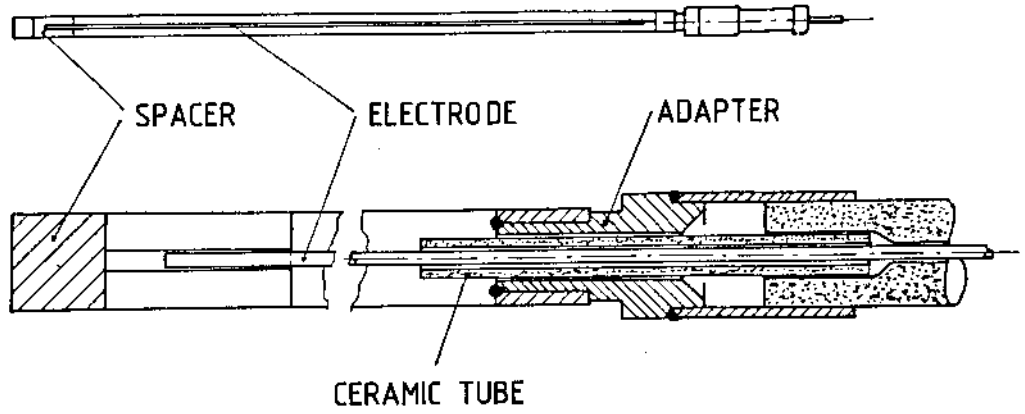
SPACER
ELECTRODE
ADAPTER
CERAMIC TUBE

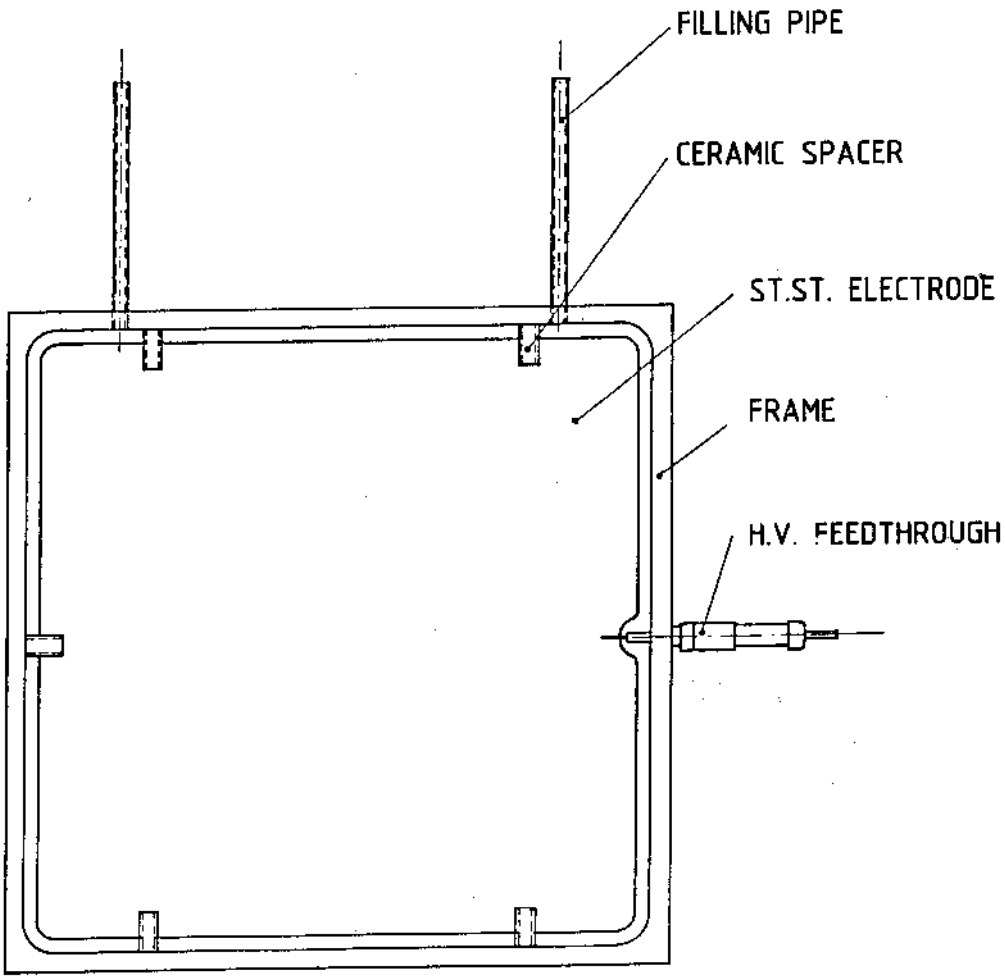
FILLING PIPE
CERAMIC SPACER
ST.ST. ELECTRODE
FRAME
H.V. FEEDTHROUGH

Figure 5

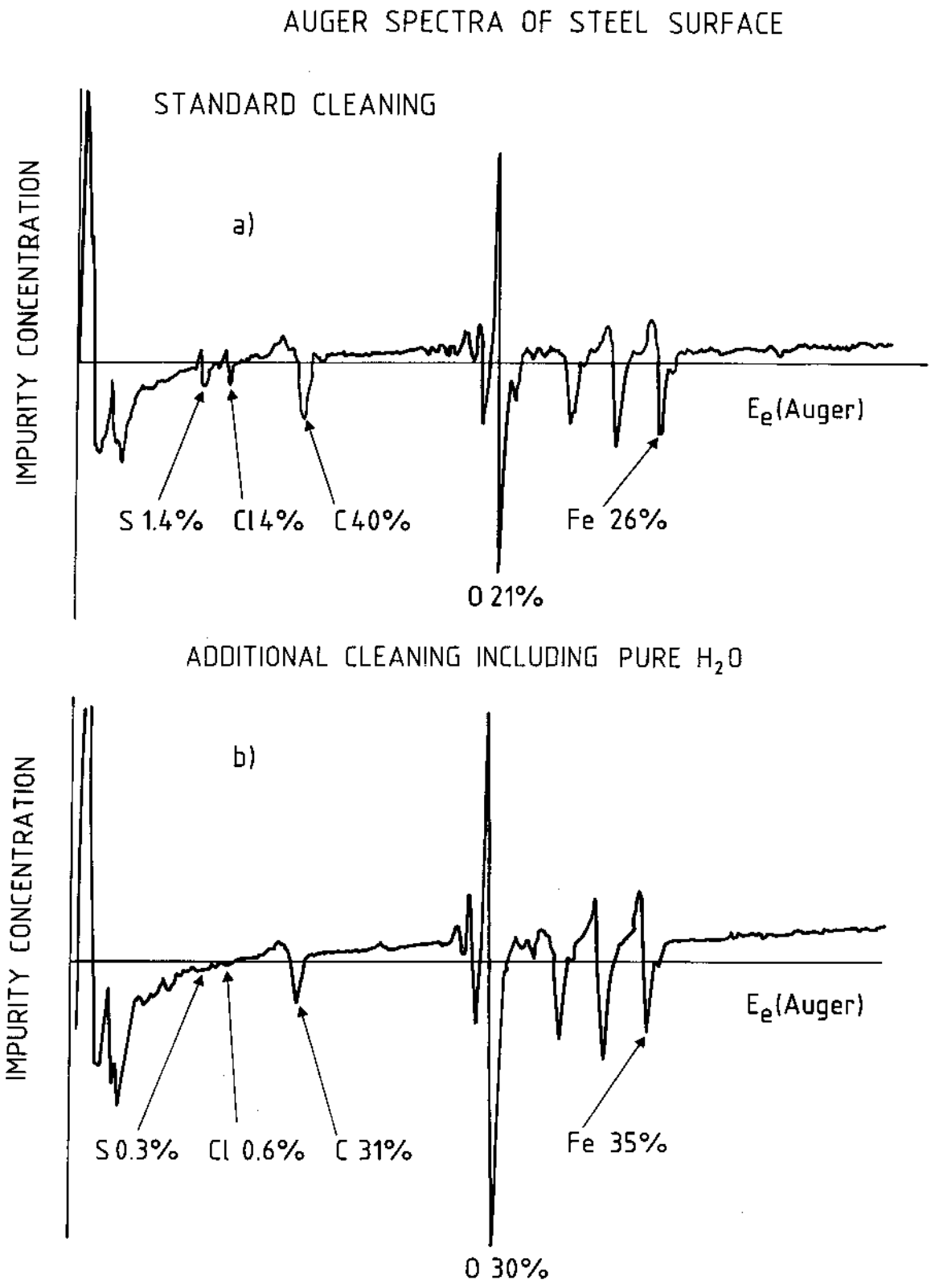
AUGER SPECTRA OF STEEL SURFACE
STANDARD CLEANING
a)
IMPURITY CONCENTRATION
E_e(Auger)
S 1.4%
Cl 4%
C 40%
O 21%
Fe 26%
ADDITIONAL CLEANING INCLUDING PURE H_2O
b)
IMPURITY CONCENTRATION
E_e(Auger)
S 0.3%
Cl 0.6%
C 31%
O 30%
Fe 35%

Figure 6

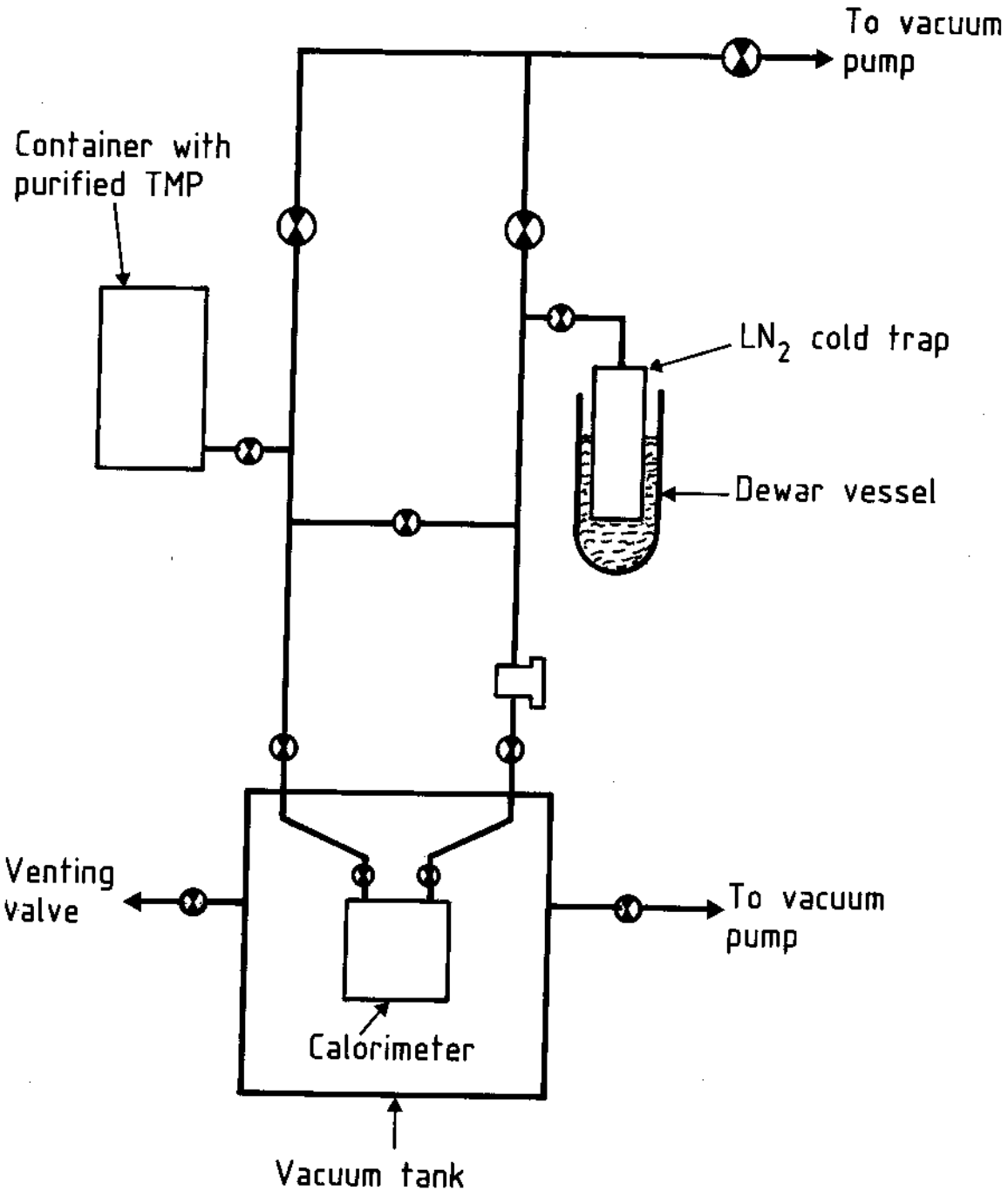
To vacuum pump
Container with purified TMP
LN_2 cold trap
Dewar vessel
Venting valve
To vacuum pump
Calorimeter
Vacuum tank

Figure 7

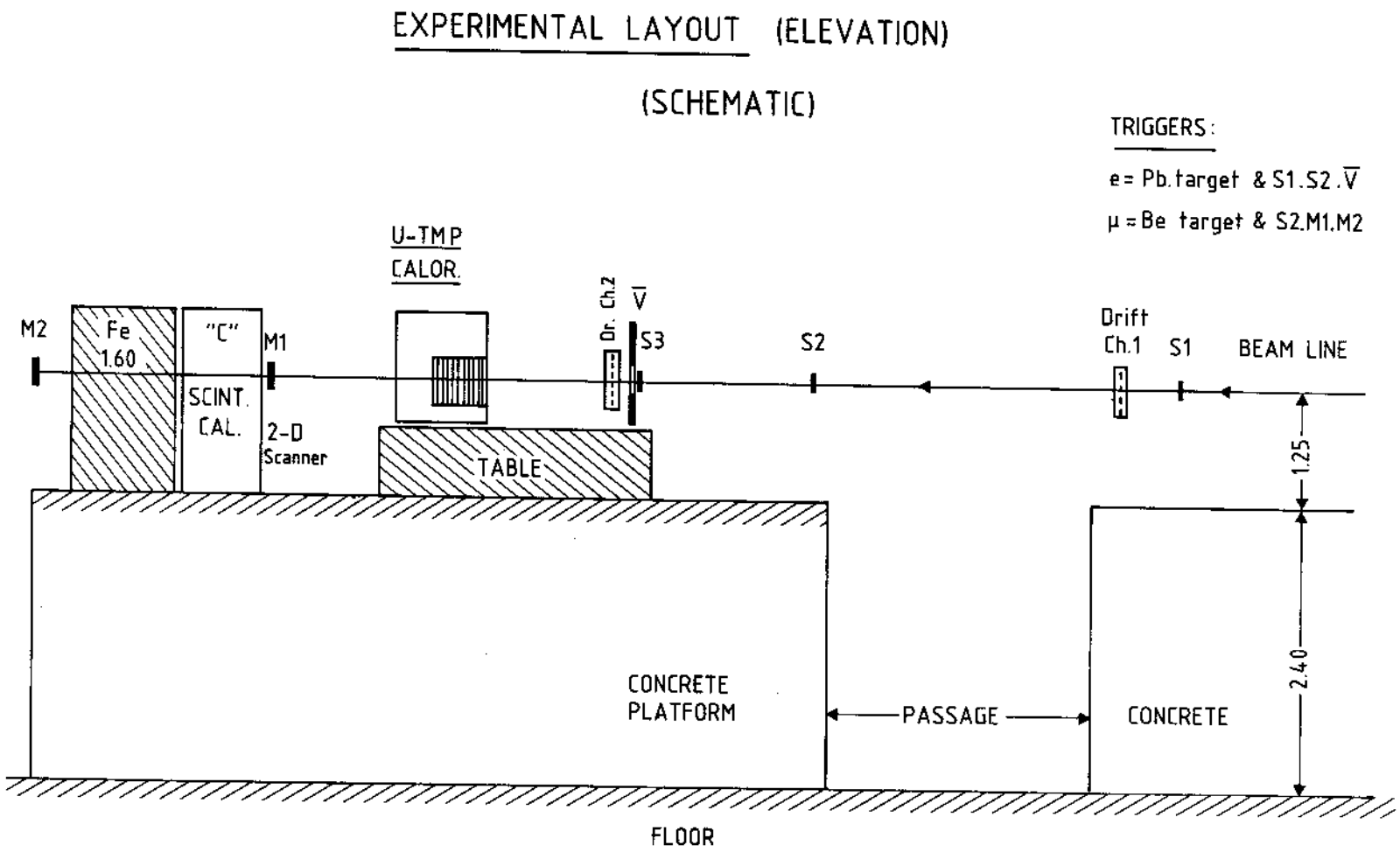
EXPERIMENTAL LAYOUT (ELEVATION)
(SCHEMATIC)
TRIGGERS:
e = Pb. target & S1.S2.$\overline{V}$
μ = Be target & S2.M1.M2
U-TMP
CALOR.
M2
Fe
1.60
"C"
SCINT.
CAL.
M1
2-D
Scanner
Dr. Ch.2
$\overline{V}$
S3
S2
Drift
Ch.1
S1
BEAM LINE
TABLE
1.25
2.40
CONCRETE
PLATFORM
PASSAGE
CONCRETE
FLOOR

Figure 8

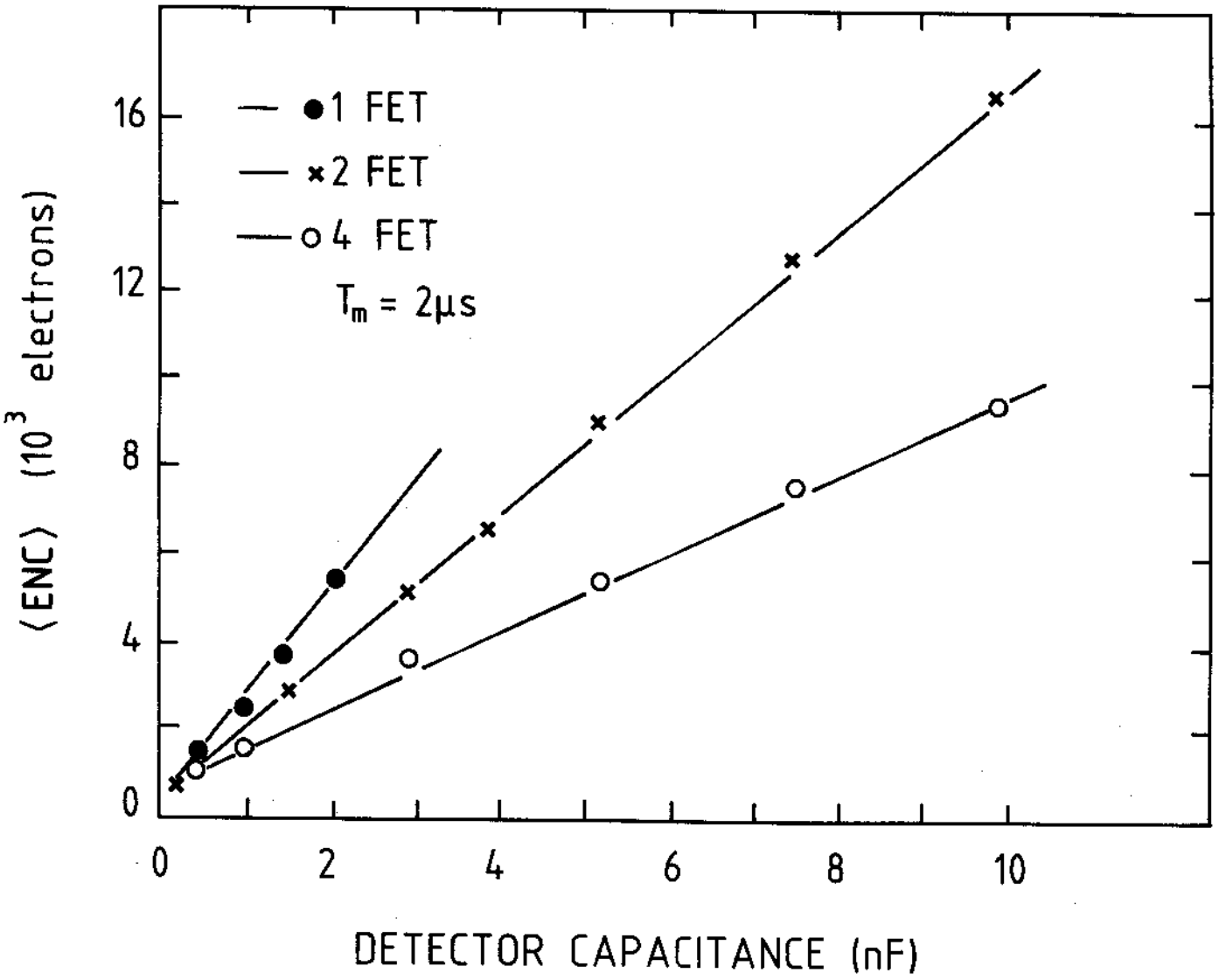
1 FET
2 FET
4 FET
T_m = 2μs
⟨ENC⟩ (10^3 electrons)
0
4
8
12
16
0
2
4
6
8
10
DETECTOR CAPACITANCE (nF)

Figure 9

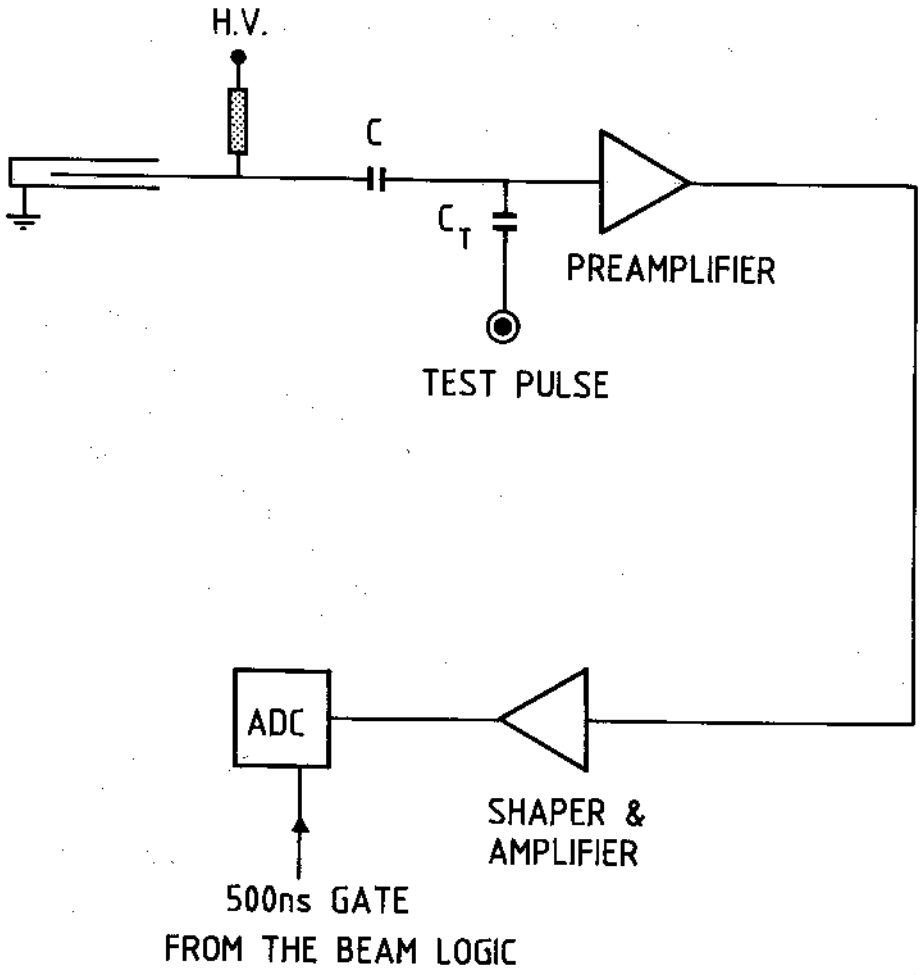
H.V.
C
C_T
PREAMPLIFIER
TEST PULSE
ADC
SHAPER &
AMPLIFIER
500ns GATE
FROM THE BEAM LOGIC

Figure 10

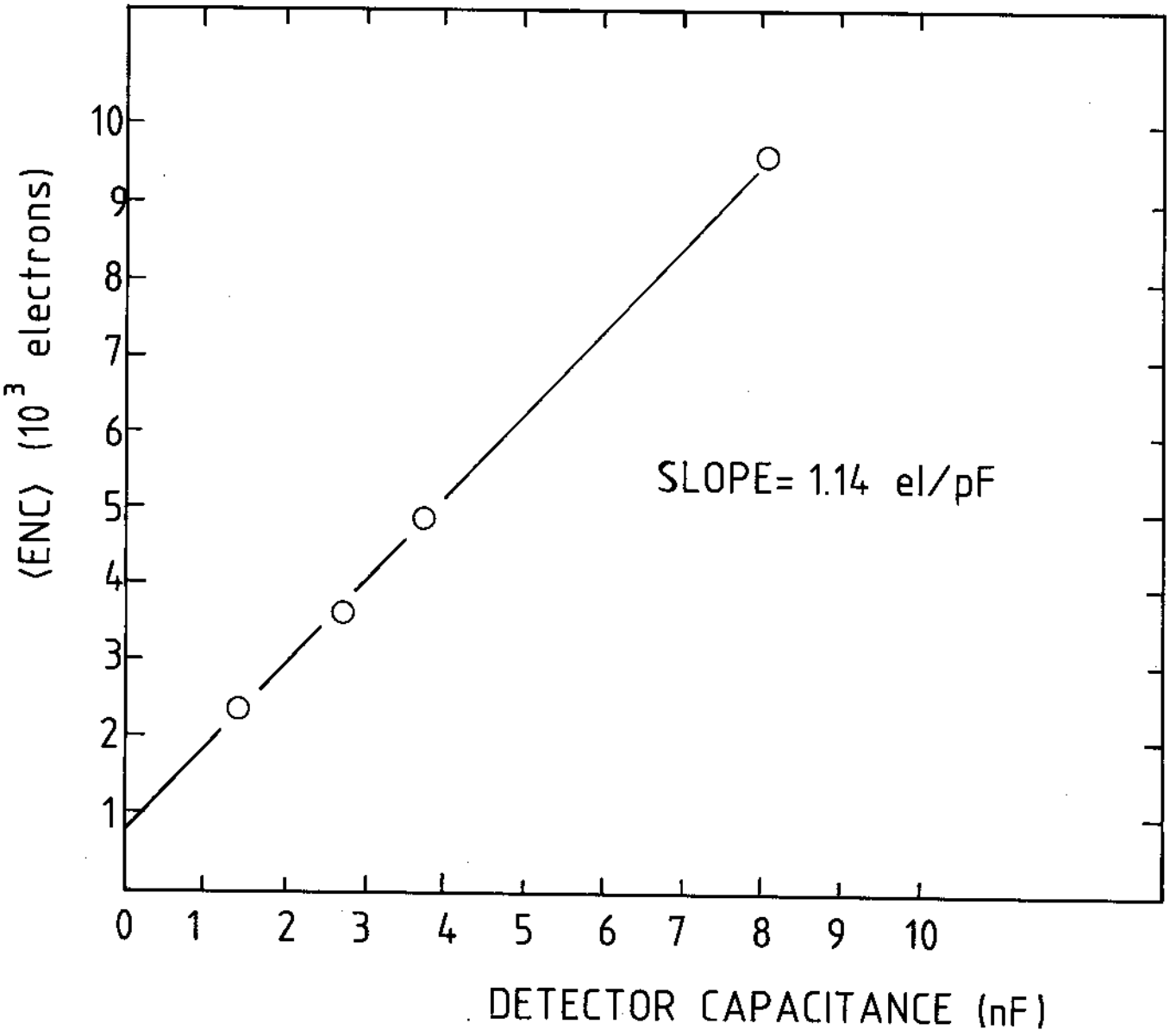
(ENC) (10^3 electrons)
10
9
8
7
6
5
4
3
2
1
0 1 2 3 4 5 6 7 8 9 10
DETECTOR CAPACITANCE (nF)
SLOPE= 1.14 el/pF

Figure 11

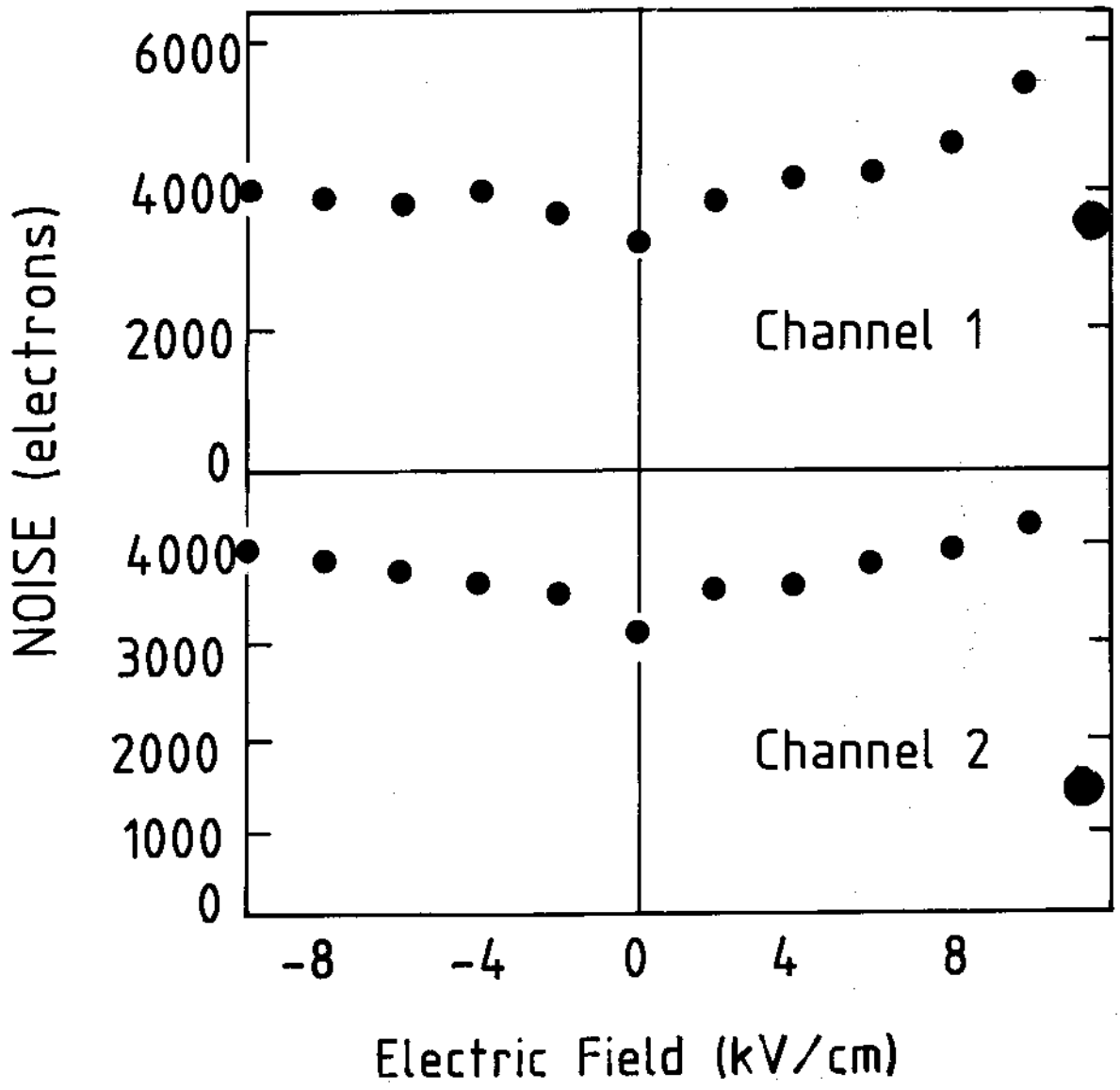
6000
4000
2000
0
Channel 1
4000
3000
2000
1000
0
Channel 2
NOISE (electrons)
-8
-4
0
4
8
Electric Field (kV/cm)

Figure 12

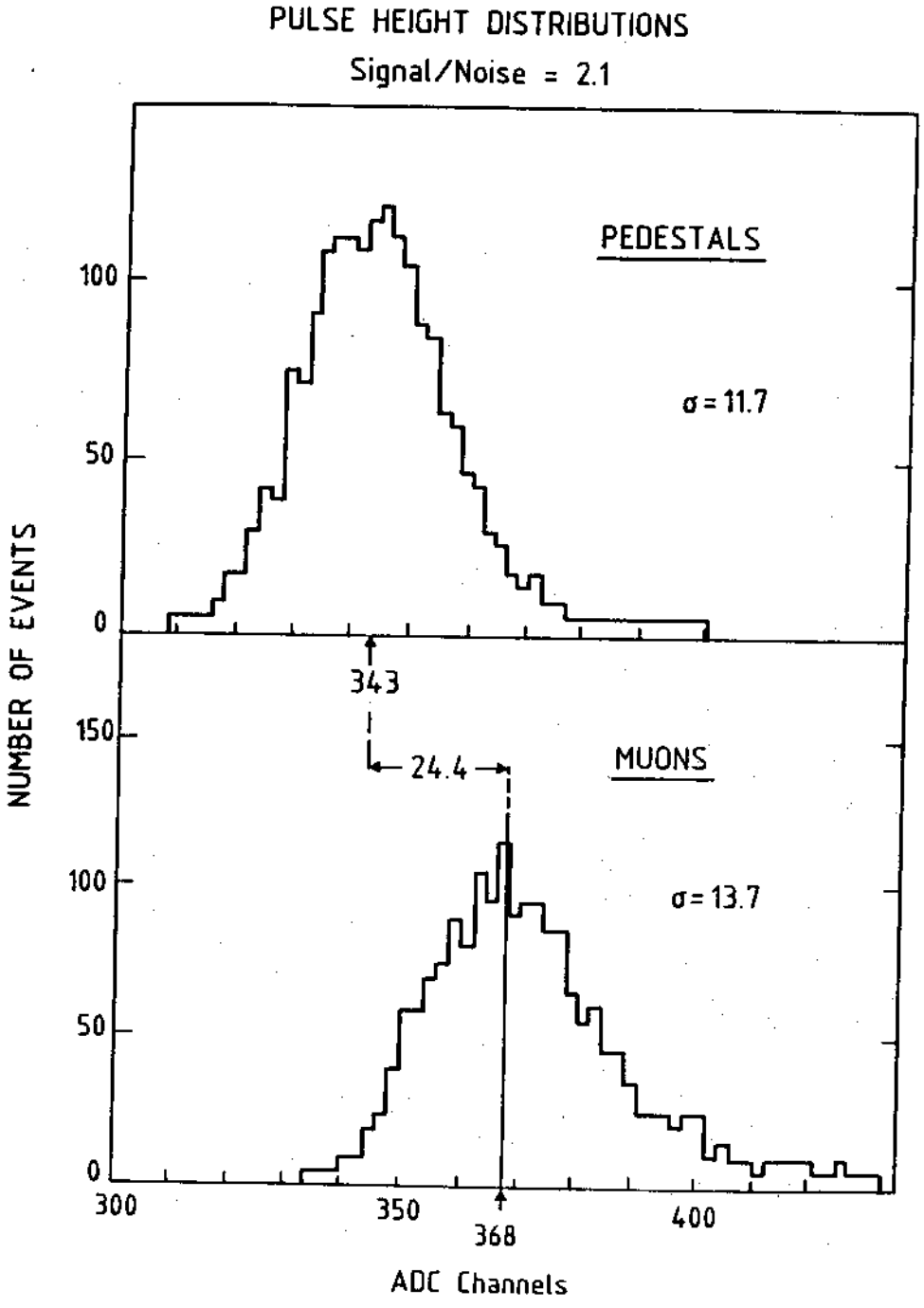
PULSE HEIGHT DISTRIBUTIONS
Signal/Noise = 2.1
PEDESTALS
σ = 11.7
MUONS
σ = 13.7
343
24.4
368
NUMBER OF EVENTS
ADC Channels
0
50
100
150
300
350
400

Figure 13

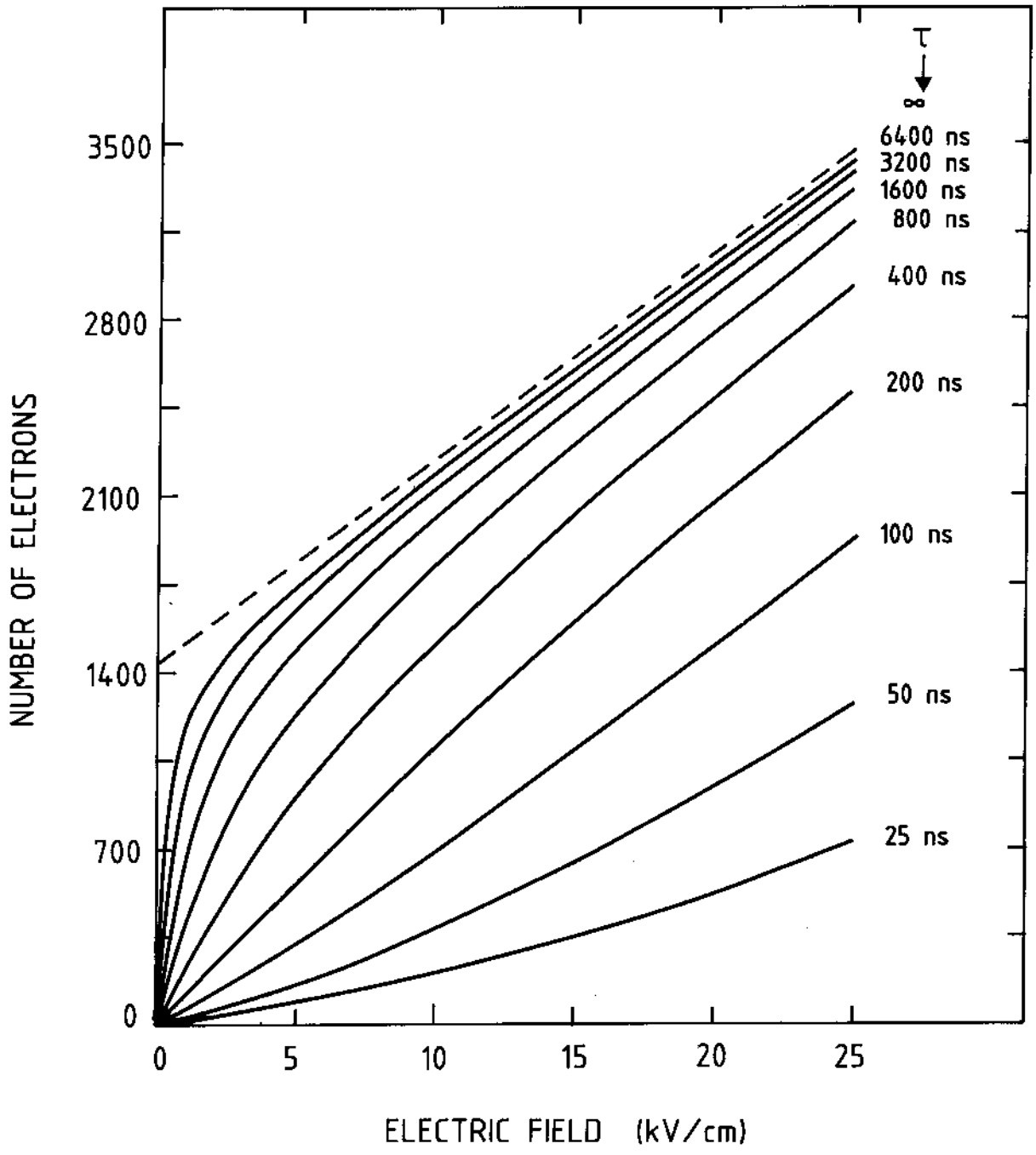
τ
∞
6400 ns
3200 ns
1600 ns
800 ns
400 ns
200 ns
100 ns
50 ns
25 ns
3500
2800
2100
1400
700
0
0
5
10
15
20
25
NUMBER OF ELECTRONS
ELECTRIC FIELD (kV/cm)

Figure 14

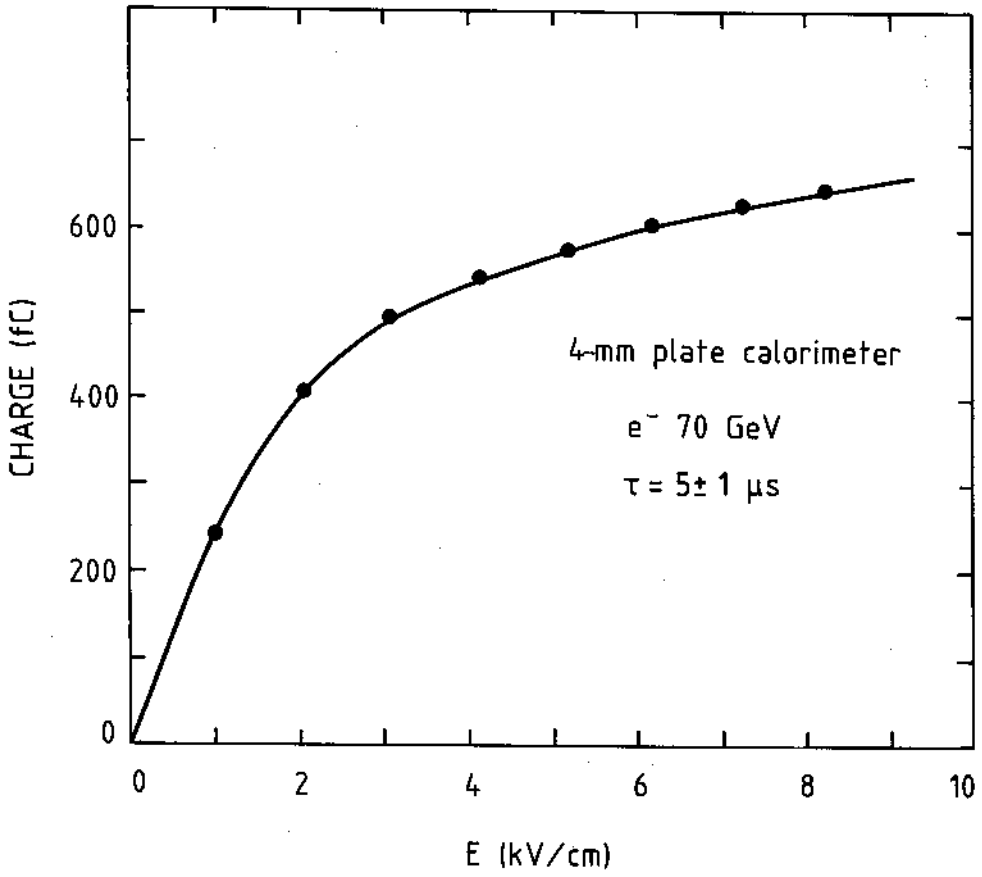

Figure 15 a

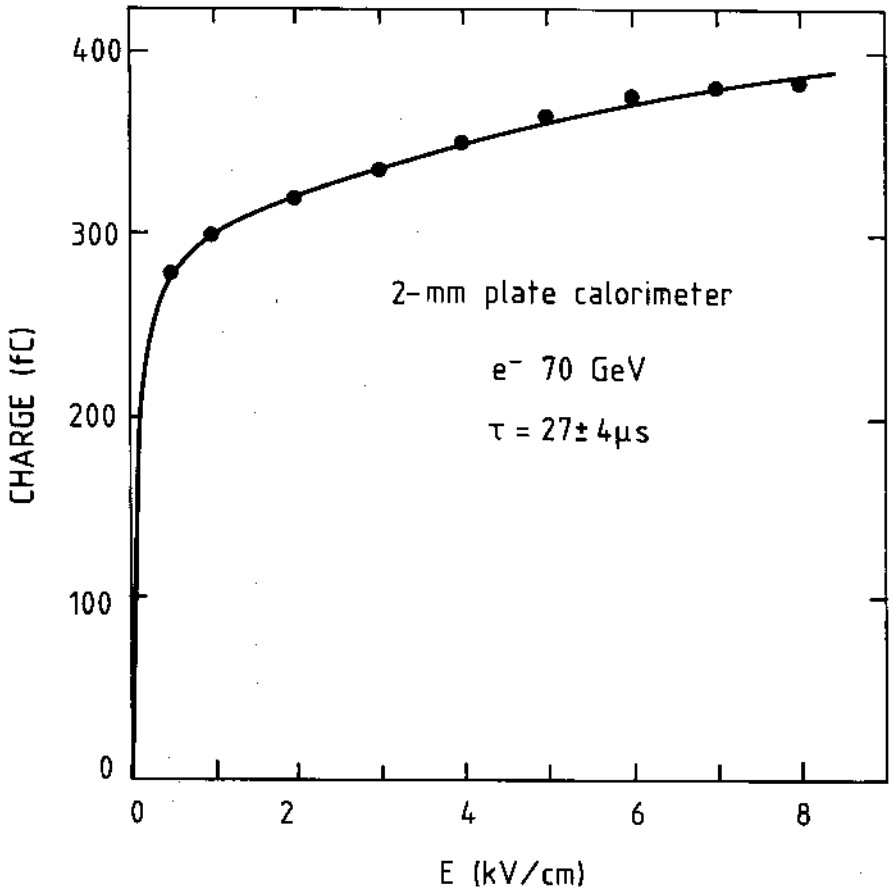

Figure 15 b

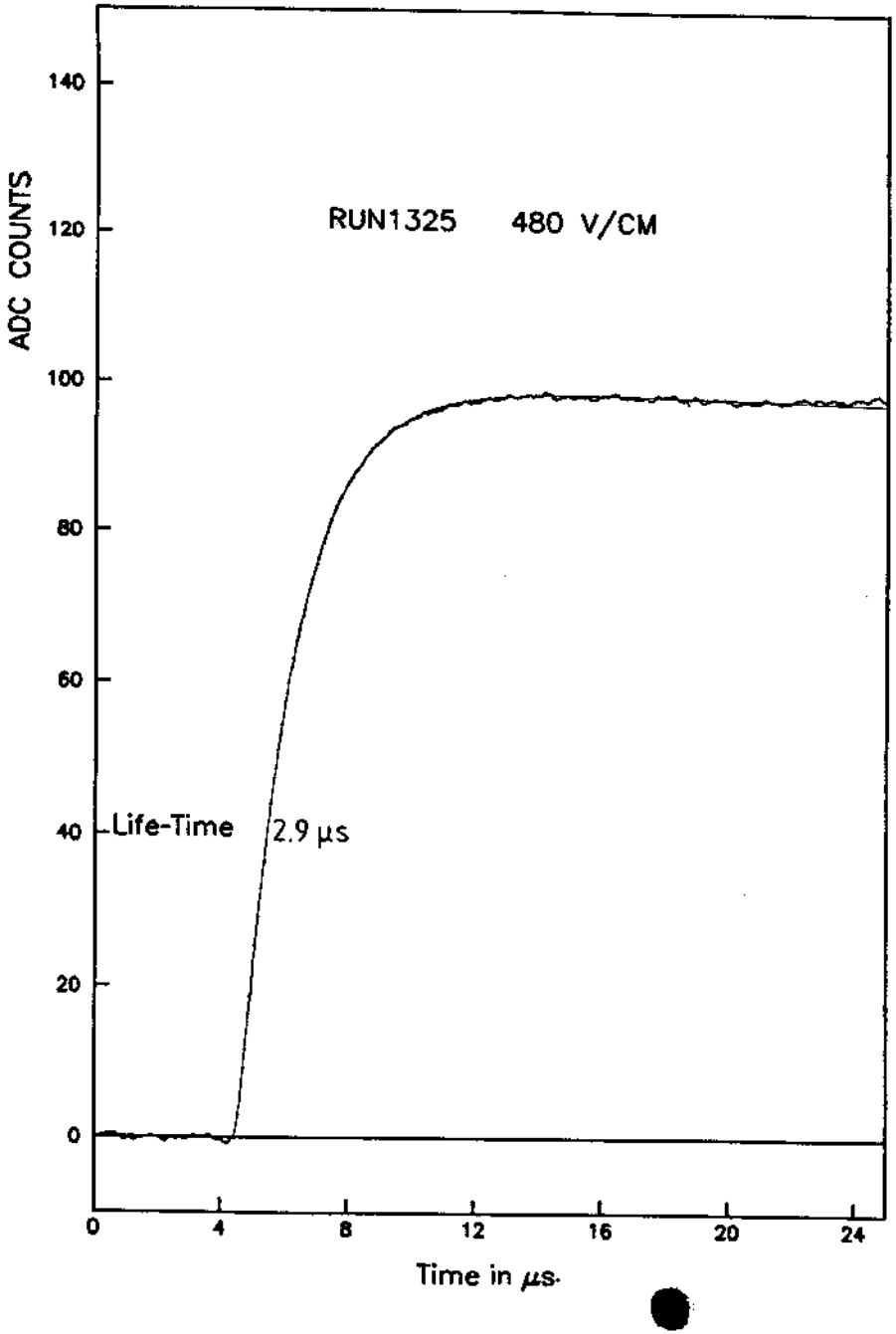

Figure 16 a

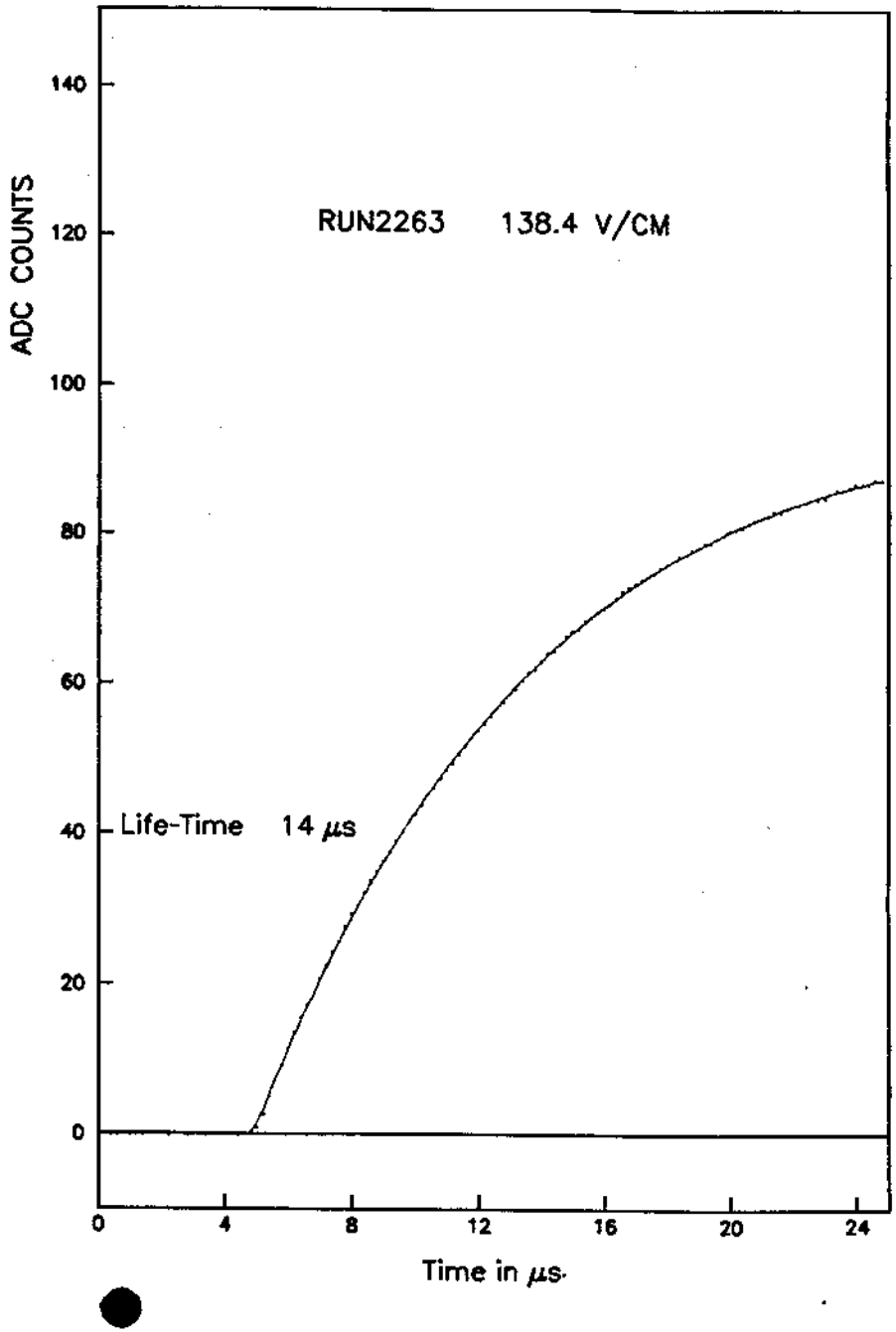

Figure 16 b

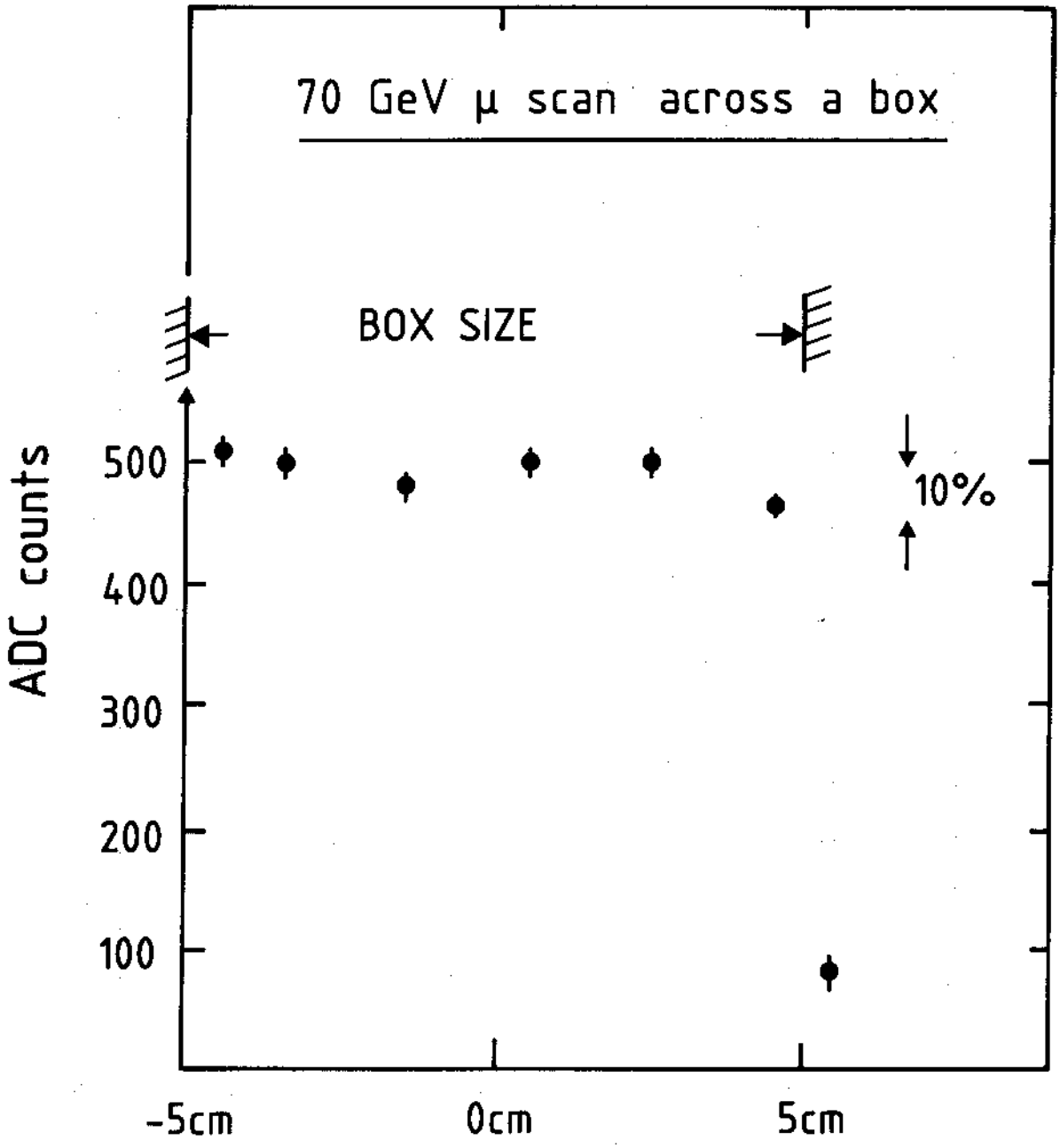
70 GeV μ scan across a box
BOX SIZE
ADC counts
500
400
300
200
100
10%
-5cm
0cm
5cm

Figure 17

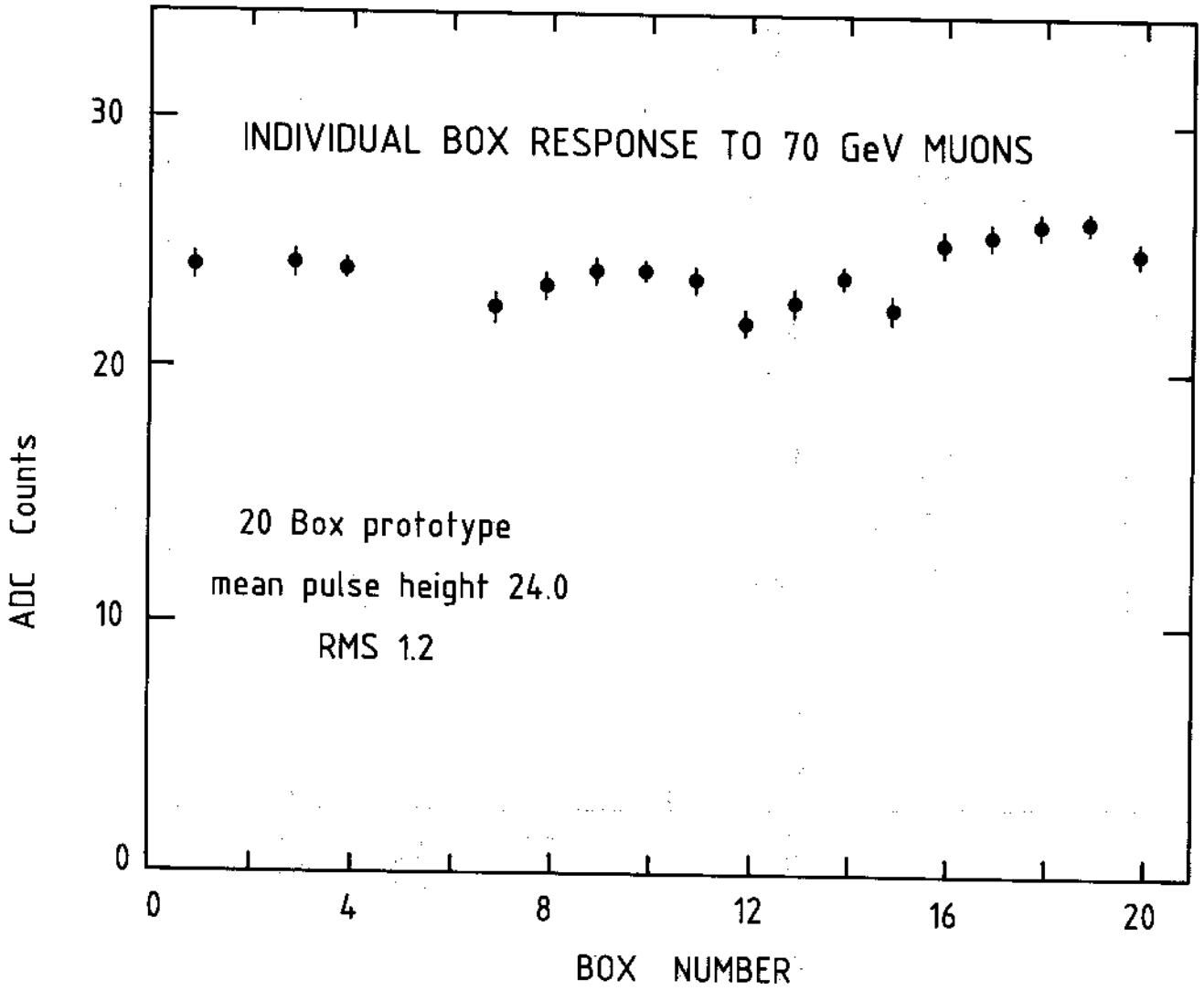
INDIVIDUAL BOX RESPONSE TO 70 GeV MUONS
20 Box prototype
mean pulse height 24.0
RMS 1.2
ADC Counts
BOX NUMBER
0
10
20
30
0
4
8
12
16
20

Figure 18

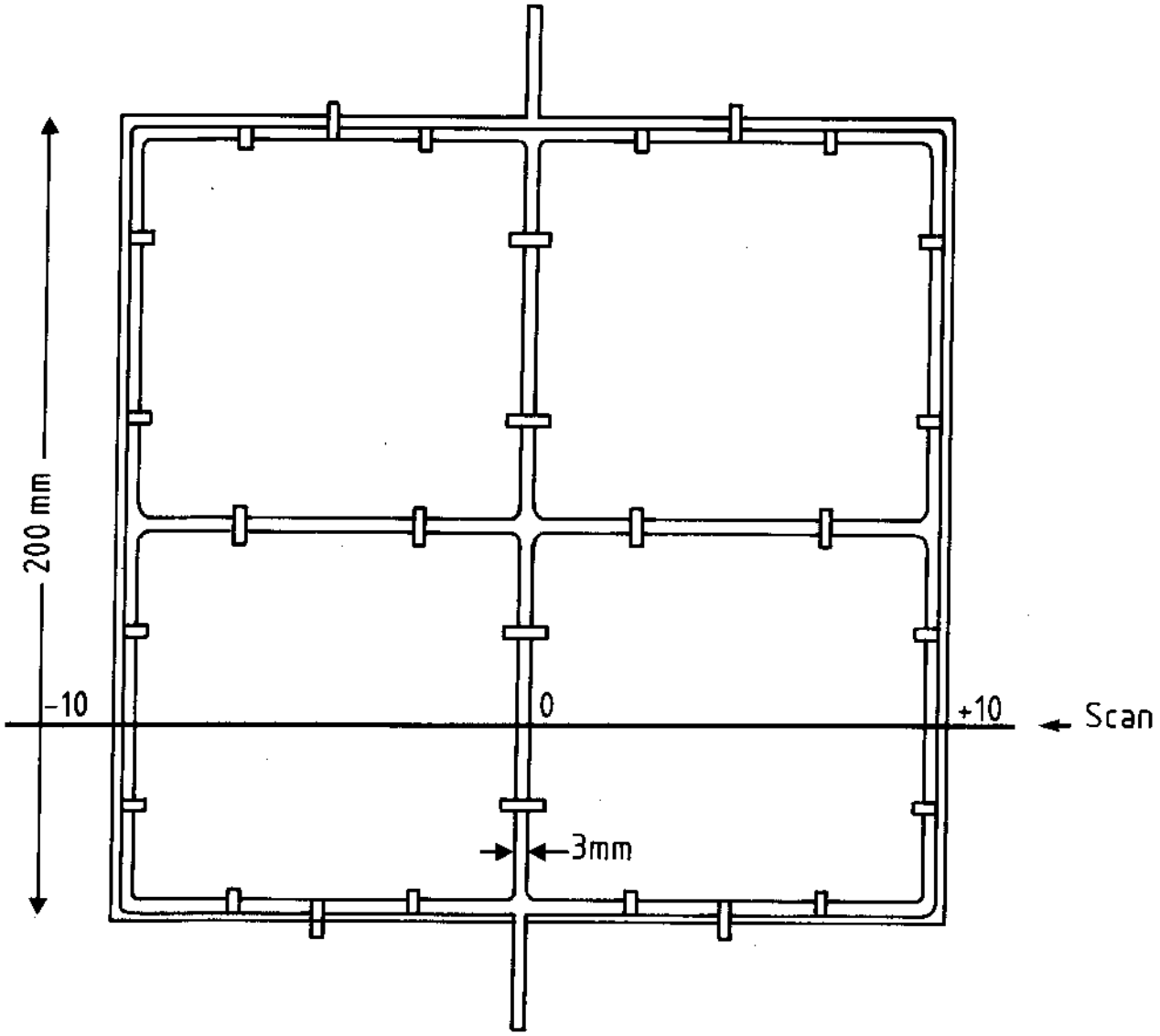

Figure 19

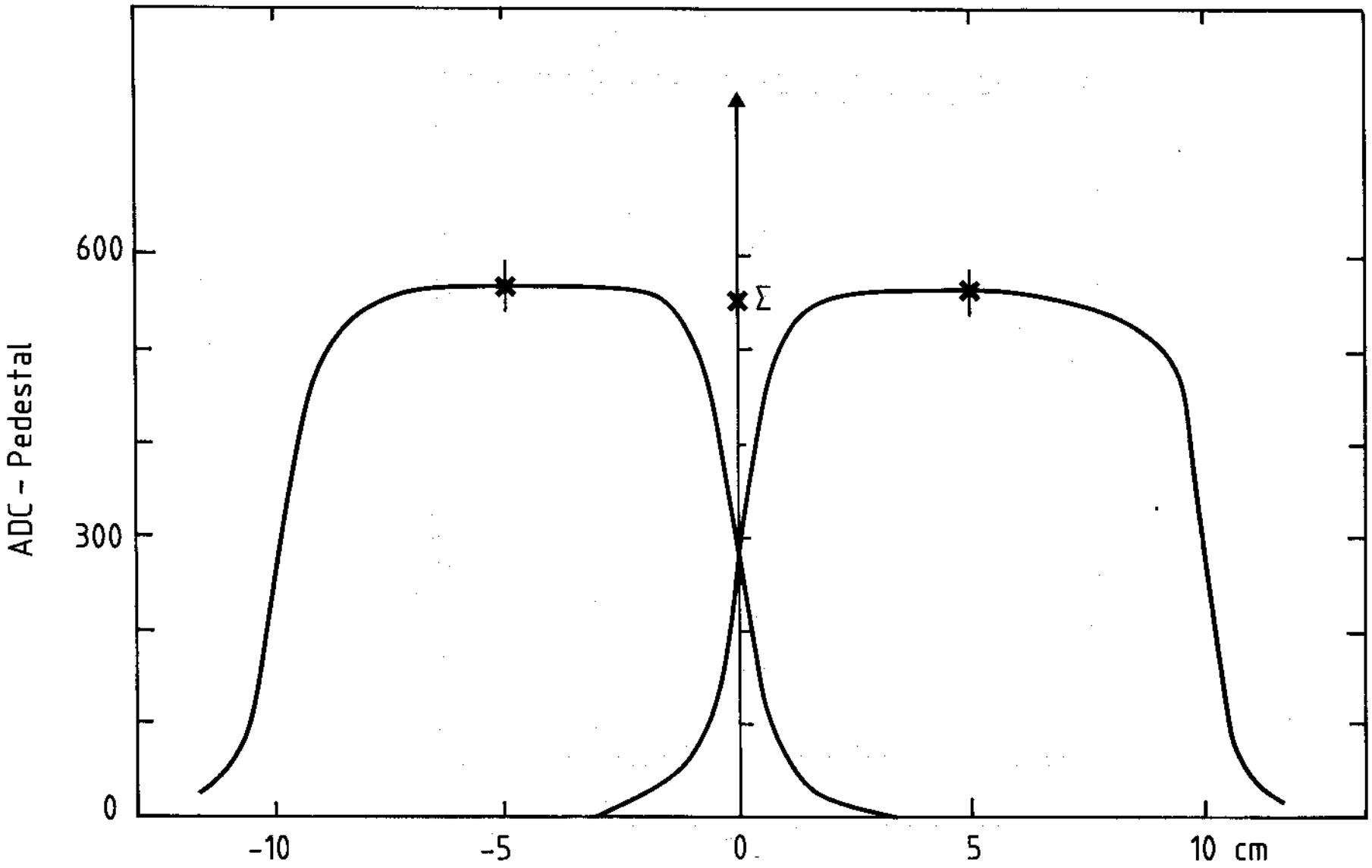

Figure 20

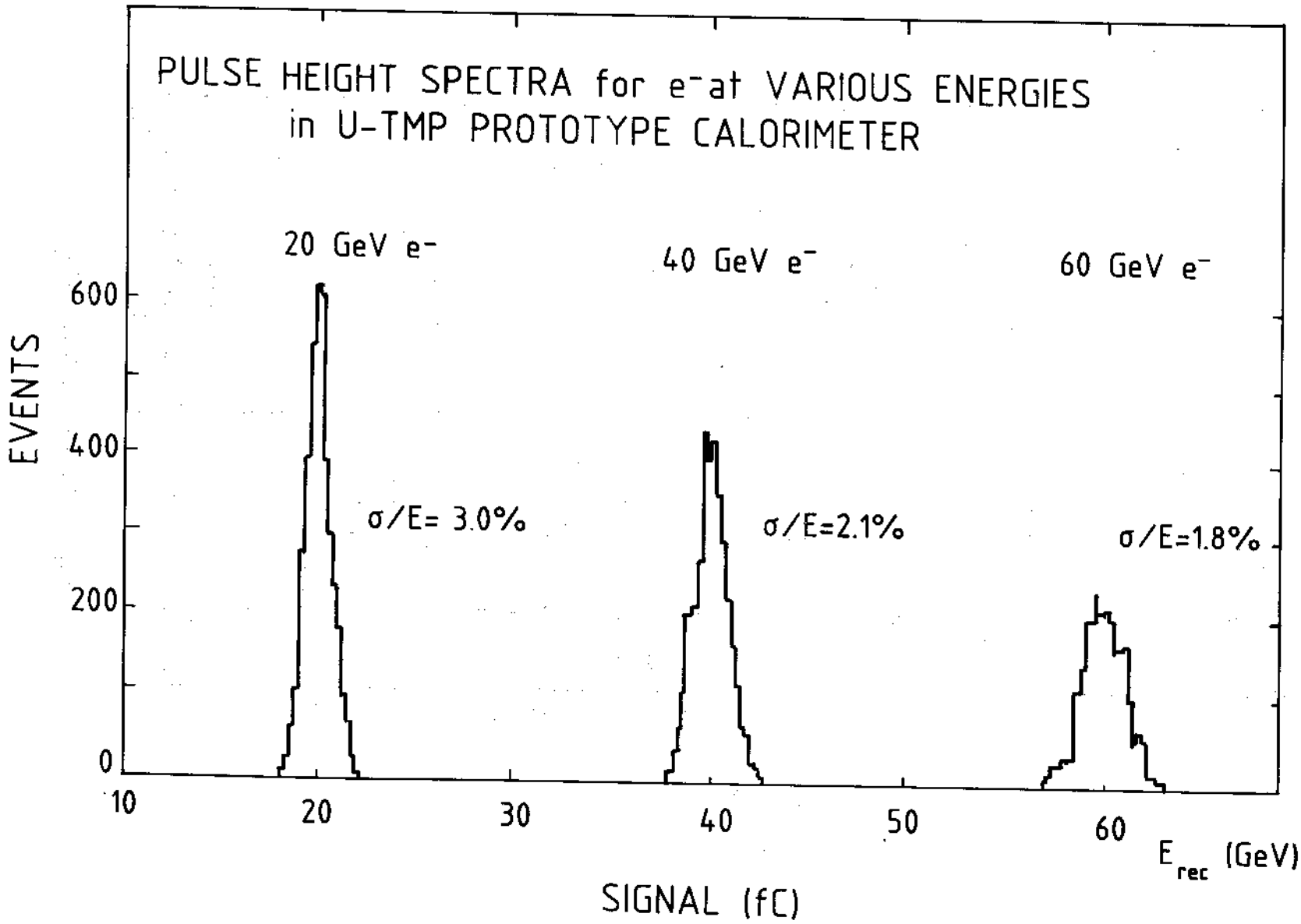
PULSE HEIGHT SPECTRA for e⁻at VARIOUS ENERGIES
in U-TMP PROTOTYPE CALORIMETER
20 GeV e⁻
40 GeV e⁻
60 GeV e⁻
σ/E= 3.0%
σ/E=2.1%
σ/E=1.8%
EVENTS
600
400
200
0
10
20
30
40
50
60
E rec (GeV)
SIGNAL (fC)

Figure 21

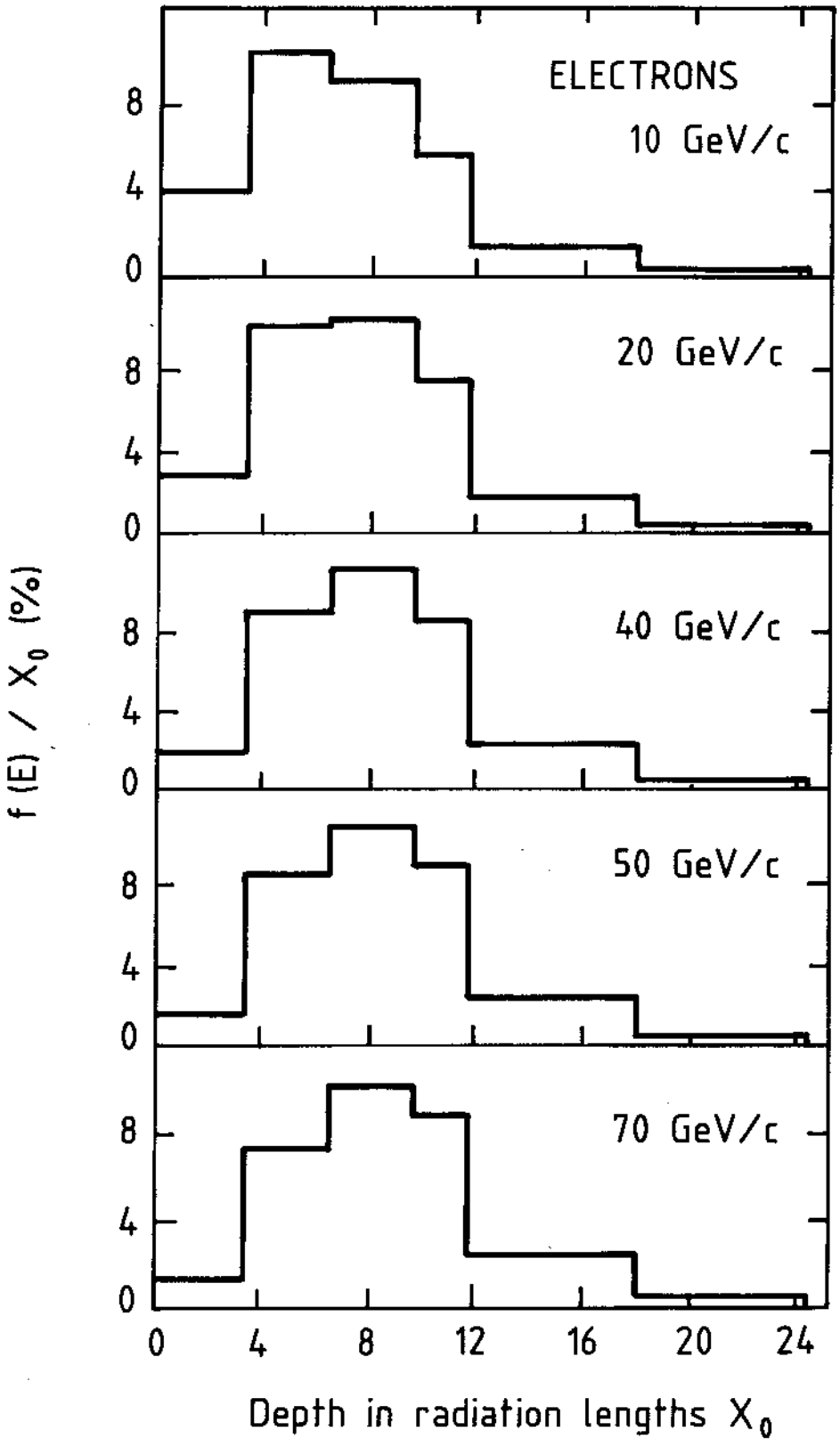
ELECTRONS
10 GeV/c
20 GeV/c
40 GeV/c
50 GeV/c
70 GeV/c
f (E) / X0 (%)
0
4
8
12
16
20
24
Depth in radiation lengths X0

Figure 22

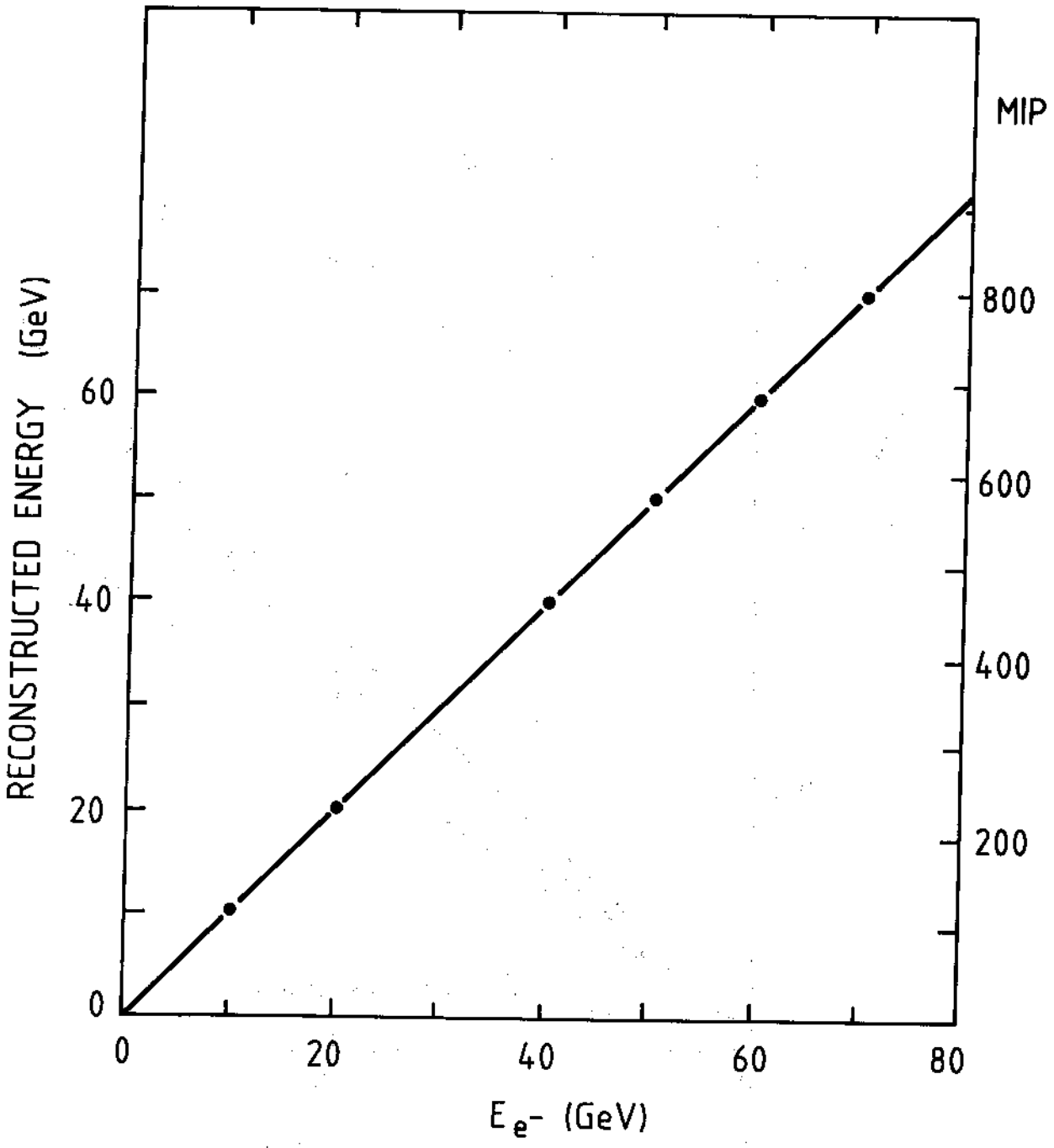
RECONSTRUCTED ENERGY (GeV)
MIP
0
20
40
60
80
200
400
600
800
0
20
40
60
E_{e^-} (GeV)

Figure 23

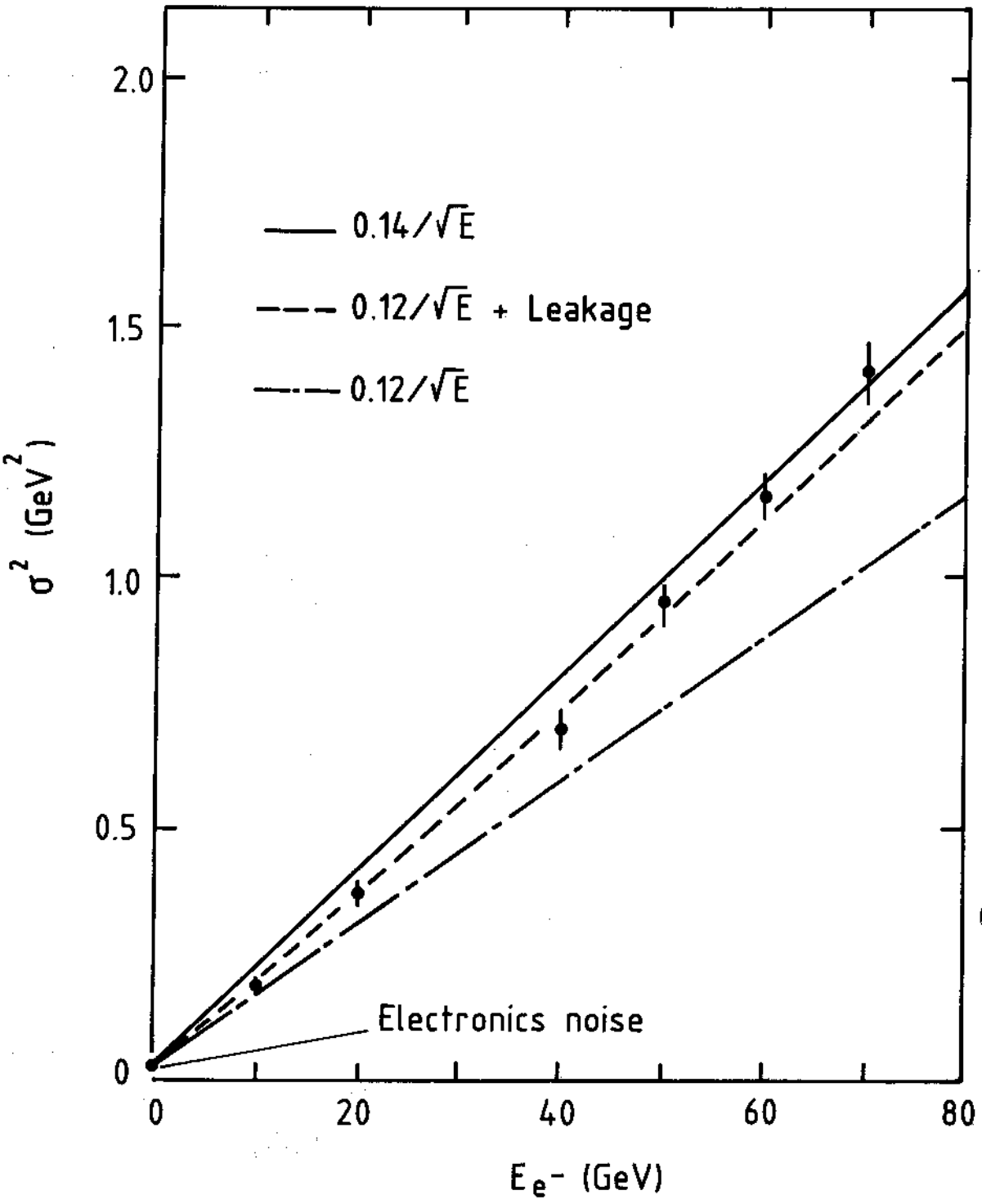
2.0
1.5
1.0
0.5
0
0.14/√E
0.12/√E + Leakage
0.12/√E
Electronics noise
σ² (GeV²)
0
20
40
60
80
E_e⁻ (GeV)

Figure 24

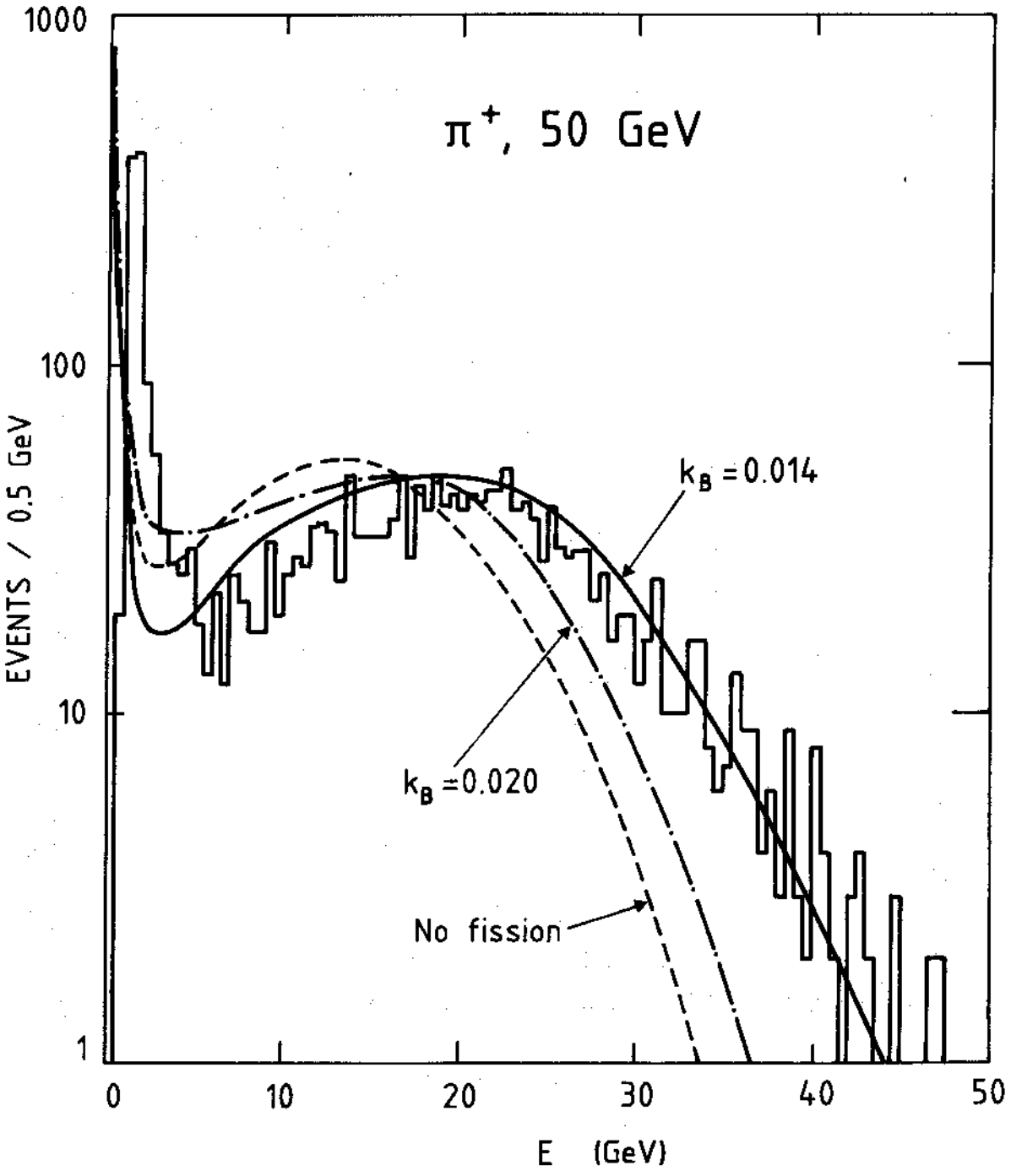
1000
100
10
1
EVENTS / 0.5 GeV
π+, 50 GeV
kB = 0.014
kB = 0.020
No fission
0
10
20
30
40
50
E (GeV)

Figure 25

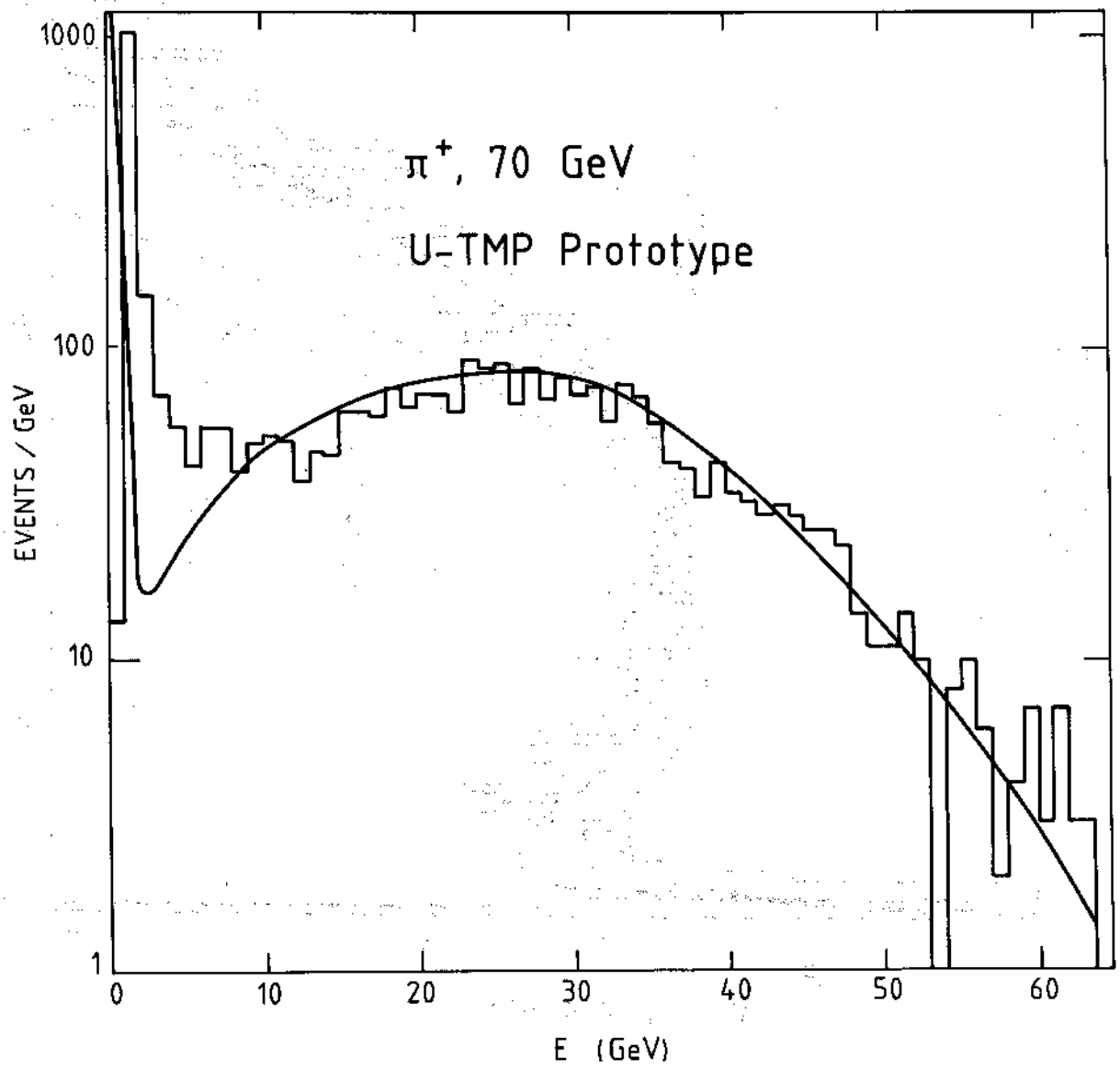
1000
100
10
1
EVENTS / GeV
π^+, 70 GeV
U-TMP Prototype
0
10
20
30
40
50
60
E (GeV)

Figure 26

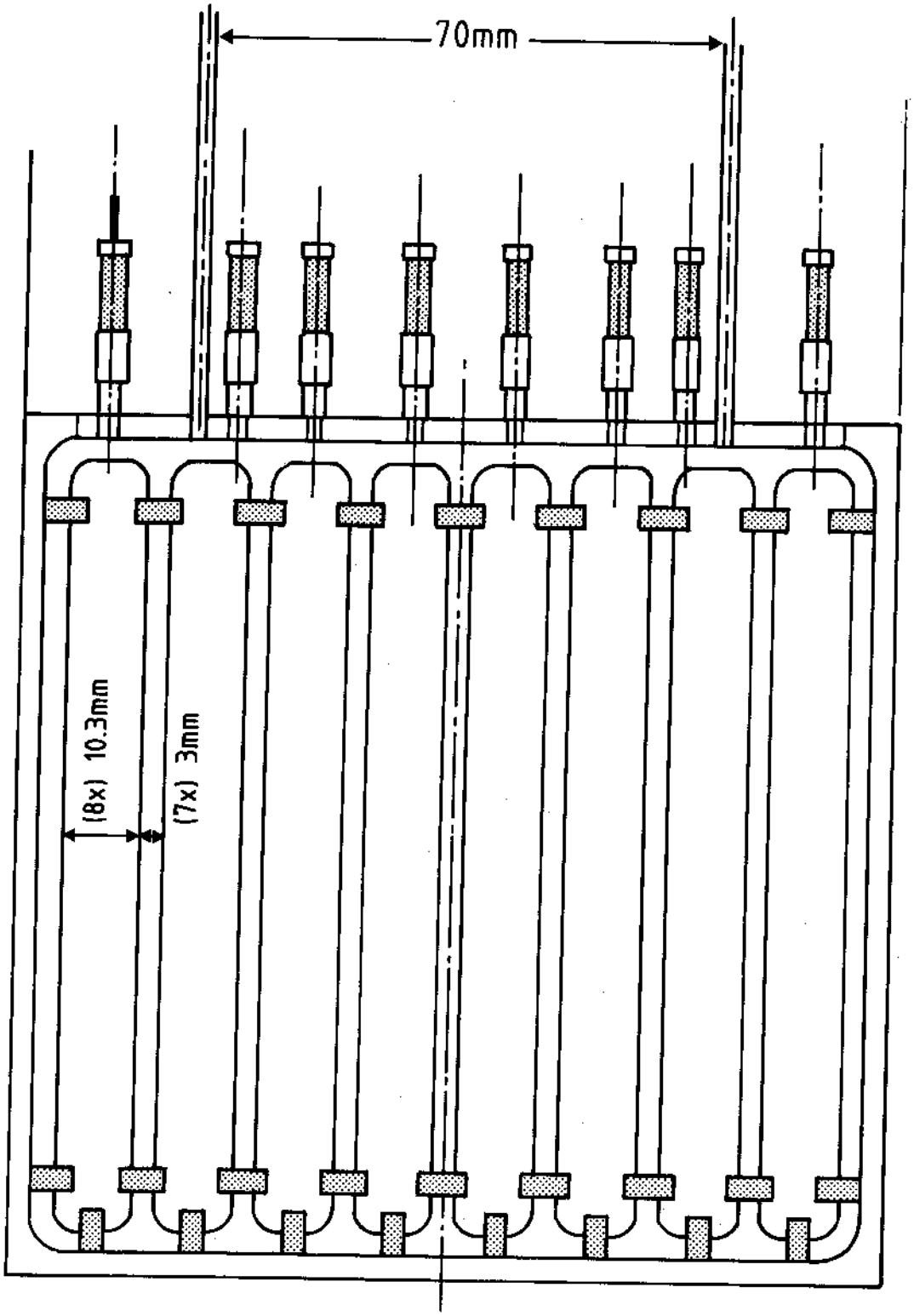

Figure 27

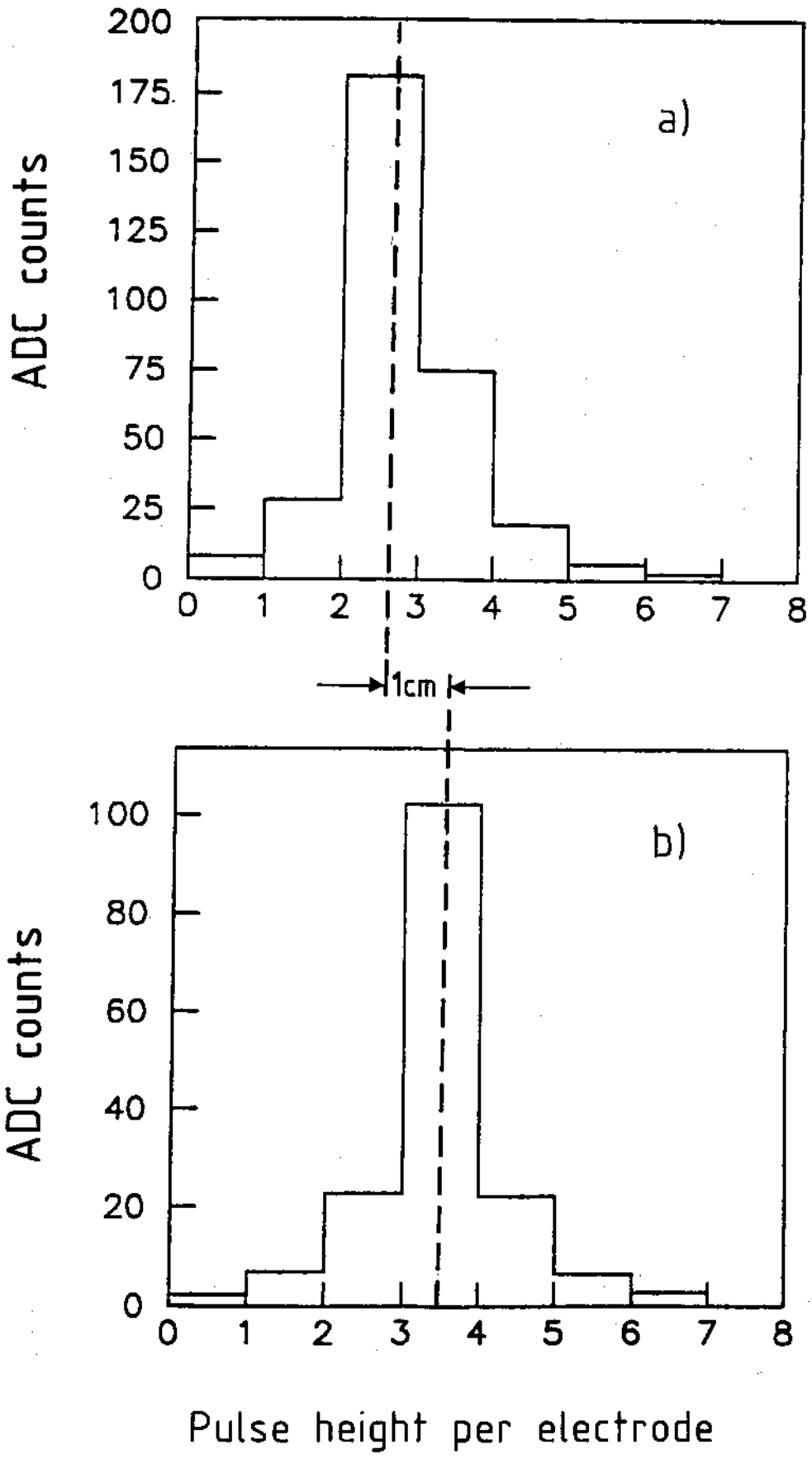
ADC counts
200
175
150
125
100
75
50
25
0
0 1 2 3 4 5 6 7 8
a)
1cm
ADC counts
100
80
60
40
20
0
0 1 2 3 4 5 6 7 8
b)
Pulse height per electrode

Figure 28

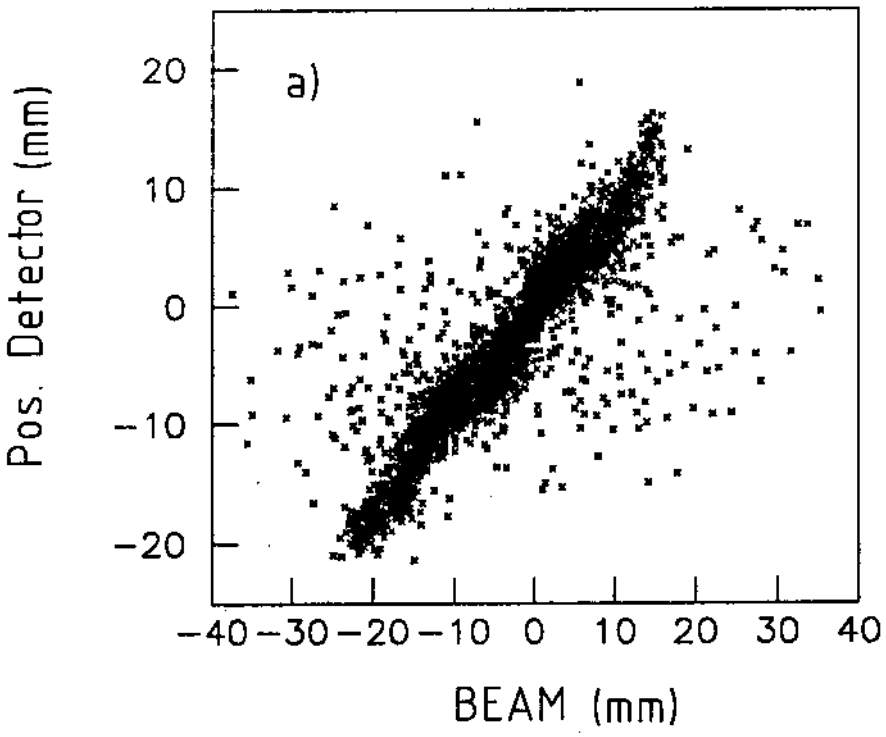
a)
Pos. Detector (mm)
20
10
0
−10
−20
−40 −30 −20 −10 0 10 20 30 40
BEAM (mm)

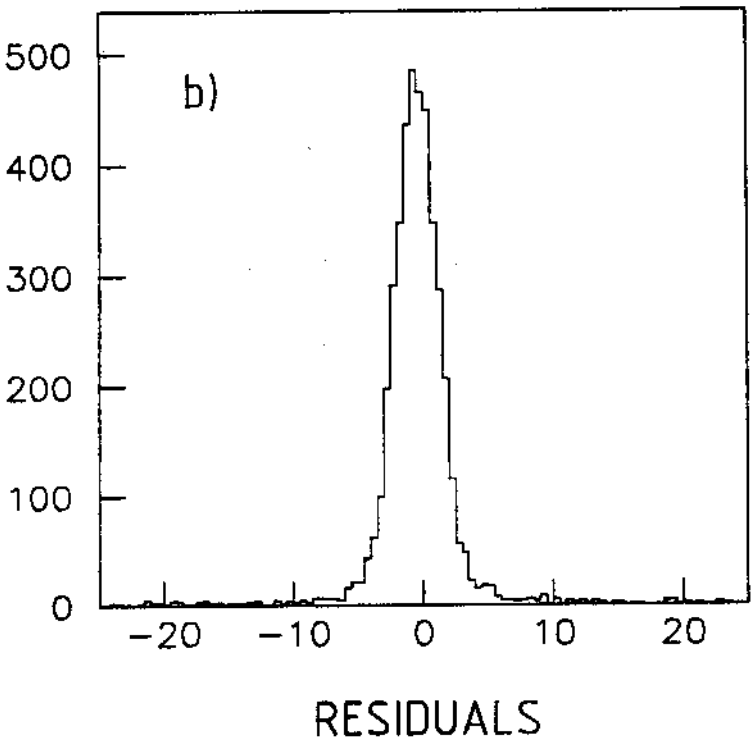
b)
500
400
300
200
100
0
−20 −10 0 10 20
RESIDUALS

Figure 29

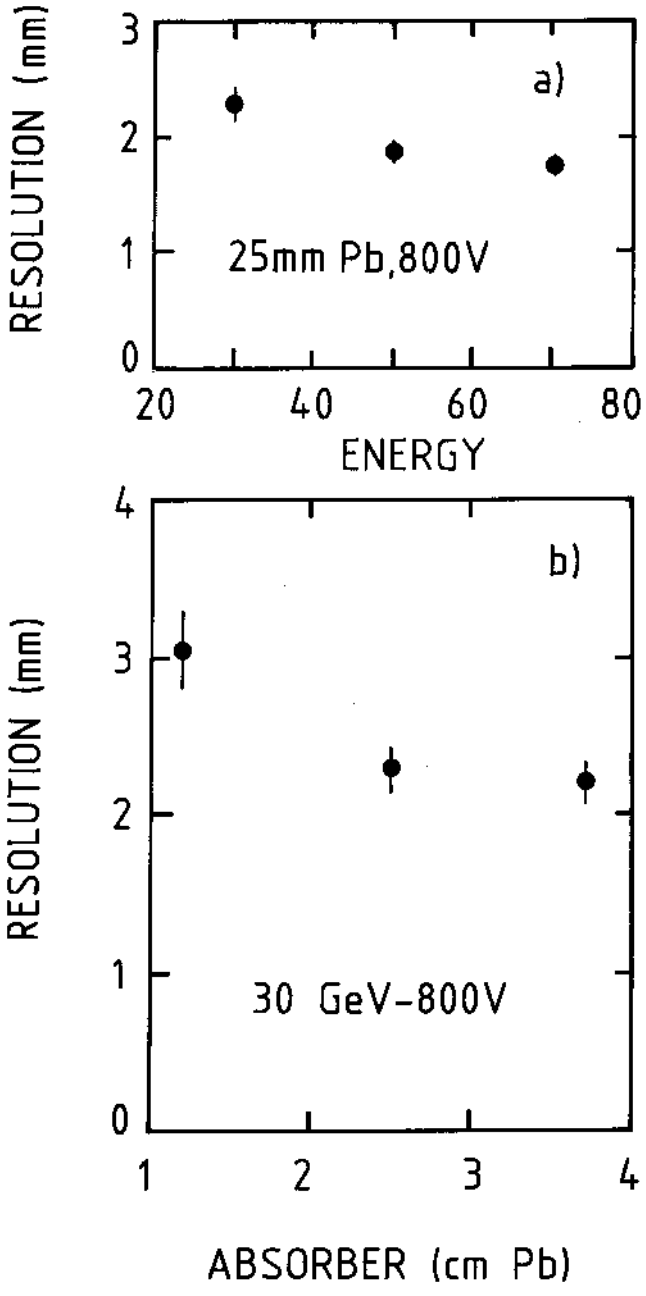
RESOLUTION (mm)
3
2
1
0
a)
25mm Pb,800V
20
40
60
80
ENERGY
RESOLUTION (mm)
4
3
2
1
0
b)
30 GeV-800V
1
2
3
4
ABSORBER (cm Pb)

Figure 30